









ORIGINAL RESEARCH

Canagliflozin Improves Myocardial Perfusion, Fibrosis, and Function in a Swine Model of Chronic Myocardial Ischemia

Sharif A. Sabe , MD; Cynthia M. Xu , MD; Mohamed Sabra , MD; Dwight Douglas Harris , MD; Akshay Malhotra ; Ahmed Aboulghheit, MD; Madigan Stanley , MD; M. Ruhul Abid , MD, PhD; Frank W. Sellke , MD

BACKGROUND: Sodium-glucose cotransporter-2 inhibitors are cardioprotective independent of glucose control, as demonstrated in animal models of acute myocardial ischemia and clinical trials. The functional and molecular mechanisms of these benefits in the setting of chronic myocardial ischemia are poorly defined. The purpose of this study is to determine the effects of canagliflozin therapy on myocardial perfusion, fibrosis, and function in a large animal model of chronic myocardial ischemia.

METHODS AND RESULTS: Yorkshire swine underwent placement of an ameroid constrictor to the left circumflex artery to induce chronic myocardial ischemia. Two weeks later, pigs received either no drug (n=8) or 300 mg sodium-glucose cotransporter-2 inhibitor canagliflozin orally, daily (n=8). Treatment continued for 5 weeks, followed by hemodynamic measurements, harvest, and tissue analysis. Canagliflozin therapy was associated with increased stroke volume and stroke work and decreased left ventricular stiffness compared with controls. The canagliflozin group had improved perfusion to ischemic myocardium compared with controls, without differences in arteriolar or capillary density. Canagliflozin was associated with decreased interstitial and perivascular fibrosis in chronically ischemic tissue, with reduced Jak/STAT (Janus kinase/signal transducer and activator of transcription) signaling compared with controls. In ischemic myocardium of the canagliflozin group, there was increased expression and activation of adenosine monophosphate-activated protein kinase, decreased activation of endothelial nitric oxide synthase, and unchanged total endothelial nitric oxide synthase. Canagliflozin therapy reduced total protein oxidation and increased expression of mitochondrial antioxidant superoxide dismutase 2 compared with controls.

CONCLUSIONS: In the setting of chronic myocardial ischemia, canagliflozin therapy improves myocardial function and perfusion to ischemic territory, without changes in collateralization. Attenuation of fibrosis via reduced Jak/STAT signaling, activation of adenosine monophosphate-activated protein kinase, and antioxidant signaling may contribute to these effects.

Key Words: canagliflozin ■ chronic myocardial ischemia ■ coronary disease ■ coronary microcirculation ■ sodium glucose cotransporter 2 inhibitor

Although surgical and catheter-based revascularization can provide significant benefit to patients with chronic coronary artery disease, a leading cause of morbidity and mortality in the United States, up to one-third of these patients are poor candidates for these interventions or receive

suboptimal revascularization.¹ Unfortunately, therapeutic options in patients with poor revascularization options remain limited. Untreated chronic myocardial ischemia contributes to myocardial necrosis, adverse remodeling, and heart failure.² Therefore, there is an ongoing need to investigate potential therapies

Correspondence to: Frank W. Sellke, MD, Division of Cardiothoracic Surgery, Department of Surgery, Cardiovascular Research Center, Rhode Island Hospital, Alpert Medical School of Brown University, 2 Dudley Street, MOC 360, Providence, RI 02905. Email: fsellke@lifespan.org

The abstract of this work was presented as an oral presentation at American Heart Association Scientific Sessions as finalist for the Vivien Thomas Young Investigator Award, November 5–7, 2022.

Supplemental Material is available at <https://www.ahajournals.org/doi/suppl/10.1161/JAHA.122.028623>

For Sources of Funding and Disclosures, see page 14.

© 2022 The Authors. Published on behalf of the American Heart Association, Inc., by Wiley. This is an open access article under the terms of the [Creative Commons Attribution-NonCommercial-NoDerivs](https://creativecommons.org/licenses/by-nc-nd/4.0/) License, which permits use and distribution in any medium, provided the original work is properly cited, the use is non-commercial and no modifications or adaptations are made.

JAHA is available at: www.ahajournals.org/journal/jaha

CLINICAL PERSPECTIVE

What Is New?

- Nondiabetic swine with chronic myocardial ischemia receiving long-term canagliflozin therapy had improved myocardial function and perfusion to ischemic territory compared with control swine.
- Canagliflozin therapy was associated with reduced left ventricular stiffness and interstitial and perivascular fibrosis, which may be secondary to reduced Jak/STAT (Janus kinase/signal transducer and activator of transcription) signaling.
- Reduced oxidative stress, activation of adenosine monophosphate-activated protein kinase signaling, and attenuation of profibrotic signaling may contribute to these effects.

What Are the Clinical Implications?

- Sodium glucose cotransporter 2 inhibitors are currently recommended for many patients with heart failure, and small animal trials suggest benefit in acute myocardial infarction, but the specific role and functional benefits of sodium glucose cotransporter 2 inhibitors in chronic coronary artery disease are ill defined in animal and clinical trials.
- Our clinically relevant large animal model of chronic myocardial ischemia provides functional and molecular mechanistic evidence of how canagliflozin therapy may exert benefit in patients with chronic coronary artery disease, warranting further investigation in this area.

Nonstandard Abbreviations and Acronyms

AMPK	5' adenosine monophosphate-activated protein kinase
eNOS	endothelial nitric oxide synthase
ERK1/2	extracellular signal-regulated kinase 1/2
MCP1	monocyte chemoattractant protein-1
SGLT2i	sodium glucose cotransporter 2 inhibitor
STAT3	signal transducer and activator of transcription 3
TUNEL	terminal deoxynucleotidyl transferase-mediated biotin–deoxyuridine triphosphate nick-end labeling

that mitigate the adverse effects of chronic myocardial ischemia.

Recent studies have shown that sodium-glucose cotransporter-2 inhibitors (SGLT2is), which were primarily used as adjunctive antihyperglycemic agents

in patients with diabetes, have cardioprotective effects independent of glucose control. In nondiabetic animal models of acute myocardial infarction and ischemia/reperfusion injury, treatment with canagliflozin, an SGLT2i, reduces infarct size,³ mitigates left ventricular systolic and diastolic dysfunction, reduces oxidative stress, and improves endothelium-dependent vasodilation.^{4,5} Possible molecular mechanisms by which SGLT2is exert beneficial effects may include activation of 5' AMPK (adenosine monophosphate-activated protein kinase), activation of endothelial nitric oxide synthase (eNOS), and antioxidant signaling,^{6,7} though these mechanisms are still poorly understood.

Clinical trials have also demonstrated beneficial effects of SGLT2i in patients with cardiovascular disease. Patients with diabetes and known cardiovascular disease treated with SGLT2is have a lower risk of the composite outcome of cardiovascular-related death, nonfatal myocardial infarction, and stroke,^{8–10} independent of glycemic control.¹¹ Further, in nondiabetic patients with heart failure with reduced or preserved ejection fraction, SGLT2is significantly reduced heart failure hospitalization and cardiovascular mortality.^{12–14} These promising results have culminated in recent guidelines that recommend SGLT2is in patients with heart failure with reduced or preserved ejection fraction irrespective of the presence of type 2 diabetes.¹⁵ In addition to providing benefit to patients with heart failure, SGLT2is may also improve left ventricular remodeling in diabetic patients with coronary artery disease.¹⁶ However, there is an overall scarcity of clinical studies investigating specific functional and molecular effects of SGLT2is in the setting of myocardial ischemia, particularly in the absence of type 2 diabetes.¹⁷ Small animal models that attempt to address these gaps in knowledge are limited to acute myocardial infarction/reperfusion models that inadequately model chronic coronary disease.

Given the beneficial effects of SGLT2is in animal models of acute myocardial ischemia and in clinical outcomes trials of patients with cardiovascular disease, but the ongoing need for studies on the specific functional and molecular effects of SGLT2is in the setting of chronic coronary disease, we sought to investigate the effects of SGLT2is in our well-established large animal model of chronic myocardial ischemia. The purpose of this study is to determine the effects of canagliflozin therapy on myocardial function, perfusion, microvessel density, and fibrosis in nondiabetic swine with chronic myocardial ischemia.

METHODS

The data that support the findings of this study are available from the corresponding author upon reasonable request.

Animal Model

Sixteen Yorkshire swine (Tufts University, Boston, MA) at age 11 weeks underwent thoracotomy for placement of an ameroid constrictor (Research Instruments SW, Escondido, CA) around the proximal left circumflex artery to induce chronic myocardial ischemia as described previously.^{18–20} Two weeks later, animals received either 300mg oral canagliflozin (Janssen Pharmaceuticals, Beerse, Belgium) daily (canagliflozin, n=8, 4 female, 4 male) or vehicle with no drug (controls, n=8, 3 female, 5 male) based on random assignment before ameroid procedure. Canagliflozin dosing was selected based on standard clinical dosing recommendations in patients and was not normalized to body weight because of rapid progression of weight in young swine. Treatment continued for 5 weeks, followed by euthanasia and myocardial harvest for analysis. All experiments were approved by the Institutional Animal Care and Use Committee of the Rhode Island Hospital (#505821), and animals were cared for in coordination with veterinary technicians at Rhode Island Hospital in compliance with the *Principles of Laboratory Animal Care* formulated by the National Society of Medical Research and the *Guide for the Care and Use of Laboratory Animals*.

Ameroid Constrictor Placement

All animals underwent placement of an ameroid constrictor (1.75–2.75mm diameter) to the proximal left circumflex artery. Pigs received aspirin (10 mg/kg) and cephalexin (30 mg/kg) orally 1 day preoperatively and 5 days postoperatively. A fentanyl patch (4 µg/kg) was placed just before surgery and maintained for a total of 72 hours. Anesthesia was induced with telazol (4.4 mg/kg) and xylazine (2.2 mg/kg) injected intramuscularly. Pigs were intubated for mechanical ventilation, and inhaled isoflurane (0.75%–3.0% minimum alveolar concentration) was administered to maintain anesthesia. A normal saline intravenous drip was started at a rate of 5 mL/kg per hour. The animals were then placed in a supine position and prepped and draped in a sterile manner. A left mini-thoracotomy was made, the pericardium was opened to expose the heart, and the left atrium was retracted to expose the left circumflex artery (LCx). The LCx was identified near its origin from the left main coronary artery. The animal was systemically heparinized (80 IU/kg), and the LCx was isolated with a vessel loop. The vessel loop was then lifted to occlude the LCx for 2 minutes as confirmed by ST or T wave changes on ECG. During occlusion, 5 mL of gold microspheres (BioPal, Worcester, MA) was injected into the left atrium. The vessel loop was relaxed to restore flow to the LCx, and ECG changes were allowed to recover to baseline. An ameroid constrictor consisting of hygroscopic casein material cased in

titanium (Research Instruments SW, Escondido, CA) was sized and placed around the LCx. The inner casein ring expands inwardly over 2 to 3 weeks to induce chronic myocardial ischemia.²¹ Nitroglycerin (1 mL) was applied topically over the vessel as needed to reverse vasospasm. The incision was closed in multiple layers. Amiodarone (10 mg/kg) was administered intravenously as needed for arrhythmias. Buprenorphine (0.03 mg/kg) was administered intramuscularly before closure.

Terminal Harvest

After 5 weeks of treatment with either 300mg canagliflozin daily or no drug, pigs underwent a terminal harvest procedure. Femoral artery access was obtained with an open incision, and a pressure catheter was inserted via a 6F sheath to monitor blood pressure. The heart was then exposed through a midline sternotomy. For blood flow analyses at rest and during pacing at 150 bpm, 5 mL of isotope-labeled microspheres was injected into the left atrium while 10 mL of blood was simultaneously withdrawn from the femoral artery catheter. For hemodynamic measurements, a pressure-volume catheter (Transonic, Ithaca, NY) was placed directly into the apex of the left ventricle via a 6F sheath. At the end of the procedure, the heart was excised, and myocardial tissue was quickly divided into 16 segments based on location with respect to the left anterior descending and left circumflex arteries. Myocardial tissue segments were air dried for microsphere analysis or snap frozen in liquid nitrogen for immunoblot analysis and frozen sectioning. The proximal circumflex artery in the area of the ameroid constrictor was inspected to determine if it was occluded.

Metabolic Parameters

Weight and length of pigs were obtained at the beginning of each surgical procedure, and body mass index was calculated. During each surgical procedure baseline blood glucose was measured, then a glucose tolerance test was performed (0.5 g/kg 50% dextrose). Blood glucose was measured at 30 and 60 minutes following dextrose administration. Blood was collected at the beginning of the harvest procedure to assess serum laboratory values, including a lipid panel and liver function tests.

Myocardial Perfusion

Myocardial perfusion was determined using isotope-labeled microspheres (Biophysics Assay Laboratory, Worcester, MA) injected at different time points. During the ameroid placement procedure, while the LCx was occluded temporarily, 5 mL of gold microspheres was injected into the left atrial appendage to determine the territory of the left ventricle perfused by the LCx.

During the harvest procedure, 5 mL of lutetium microspheres was injected into the left atrium while simultaneously withdrawing 10 mL of blood from the femoral artery at a reference rate of 6.67 mL/min using a withdrawal pump (Harvard Apparatus, Holliston, MA). This protocol was repeated during pacing at 150 bpm using samarium microspheres. Blood samples and left ventricular myocardial samples from 10 sections based on proximity of location to the left anterior descending and LCx arteries were weighed, dried, and sent to Biophysics Assay laboratory for microsphere density measurements. Blood flow was calculated using the following equation: tissue blood flow = [reference blood flow (mL/min)/tissue weight (g)] \times [tissue microsphere count/reference blood microsphere count].

Hemodynamic Measurements

During the harvest procedure, a pressure catheter (Transonic, Ithica, NY) was inserted into the left femoral artery and advanced into the aorta for measurement of mean arterial pressure. A pressure volume catheter (Transonic, Ithica, NY) was inserted directly into the apex of the left ventricle for cardiac hemodynamic measurements. Load-dependent data were collected during breath holds to minimize the effect of respiratory

variation, and load-independent data were collected during breath hold and inferior vena cava occlusion with a vessel loop. Hemodynamic data were recorded and analyzed with LabChart software (ADInstruments, Colorado Springs, CO). The left ventricular stiffness constant (β) was derived from the end-diastolic pressure volume relationship.

Immunofluorescence

Immunofluorescence staining was performed as previously described.²² Briefly, frozen section slides were thawed, fixed with 10% paraformaldehyde, blocked in 3% bovine serum albumin, and incubated with primary antibody to α -SMA (alpha smooth muscle actin) (Abcam, Cambridge, UK) and isolectin B4 conjugated to Alexa Fluor 647 (Thermo Fisher Scientific, Waltham, MA) overnight at 4 °C. Slides were then rinsed 3 times with PBS, and antimouse secondary antibody conjugated to Alexa Fluor 594 (Cell Signaling, Danvers, MA) was applied and allowed to incubate for 1 hour at room temperature. After rinsing, DAPI was applied for 5 minutes, and slides were rinsed and mounted. Images were analyzed at 20 \times magnification with an Olympus VS200 Slide Scanner (Olympus Corporation, Tokyo, Japan). Image analysis was performed with QuPath

Table 1. Metabolic Parameters

Metabolic parameter	Controls	IQR	Canagliflozin	IQR	P value
BMI at ameroid, kg/m ²	58.8	52.2, 66.2	62.4	60.3, 65.0	0.72
BMI at harvest, kg/m ²	64.4	56.7, 71.4	70.3	65.6, 74.1	0.23
% change BMI	6.4	-1.9, 13.6	12.3	5.4, 19.7	0.38
BG – Baseline, mg/dL	119.5	111, 129.5	119.5	117.3, 132.8	0.75
BG – 30min post-dextrose, mg/dL	259.5	247, 279	255	233, 268	0.64
BG – 60min post-dextrose, mg/dL	243.5	214.8, 258.3	194	175.8, 248.5	0.32
Albumin, g/dL	2.6	2.4, 2.8	3.0	2.8, 3.1	0.04*
Total bilirubin, mg/dL	0.1	0.1, 0.1	0.1	0.1, 0.1	0.38
Direct bilirubin, mg/dL	0.1	0.1, 0.1	0.1	0.1, 0.1	1
Alkaline phosphatase, IU/L	134.5	119, 152	101.5	79, 127.5	0.08
Total protein, g/dL	4.7	4.6, 5.1	5.6	5.5, 5.8	0.001*
ALT, IU/L	53	52, 55.5	56	49.8, 59.3	0.53
AST, IU/L	19	17.5, 23.5	20	17.8, 21.3	0.96
Total cholesterol, mg/dL	69.5	57.8, 76.8	77.5	75.5, 80.0	0.14
Triglycerides, mg/dL	17	14.8, 21.5	11	11, 13.5	0.09
HDL, mg/dL	36.5	32, 41.5	40.5	34.8, 42.0	0.79
LDL, mg/dL	30	21, 33.5	35.5	35.0, 36.5	0.02*
CRP, mg/L	0.2	0.20, 0.36	0.37	0.28, 0.48	0.13
HbA1c, %	3	3, 3.3	3.9	3.3, 4.0	0.14

There were no significant differences in BMI at the time of ameroid procedure, harvest procedure, or in the percent change of BMI between ameroid to harvest procedure in canagliflozin-treated pigs (n=8), compared with controls (n=8). There were no significant differences in BG at baseline, and at 30 and 60 min following dextrose challenge. There was a significant increase in serum albumin, total protein, and LDL in the canagliflozin-treated pigs, compared with the control pigs. There were no differences in total or direct bilirubin, alkaline phosphatase, total protein, ALT, total AST, total cholesterol, triglycerides, HDL, CRP, or HbA1c between groups.

ALT indicates alanine aminotransferase; AST, aspartate aminotransferase; BG, blood glucose; BMI, body mass index; CRP, C-reactive protein; HbA1c, hemoglobin A1c; HDL, high-density lipoprotein; IQR, interquartile range; and LDL, low-density lipoprotein.

*P<0.05.

software in a blinded fashion.²³ Capillary density was determined by defining positive isolectin B4 staining by thresholding and determining percentage of tissue area stained. Arteriolar count was determined by defining positive SMA staining by thresholding and determining the number of objects with a minimum size of $100\mu\text{m}^2$ per area of tissue section.

Immunohistochemistry

Frozen tissue sections were prepared and mounted on slides for trichrome Masson staining or DAB TUNEL (terminal deoxynucleotidyl transferase–mediated biotin–deoxyuridine triphosphate nick-end labeling) staining as performed by iHisto (Salem, MA). Images were acquired at $20\times$ magnification using the Motic EASYS CAN Infinity brightfield slide scanner (Motic, Kowloon, Hong Kong). QuPath software was used to quantify positive trichrome staining, interstitial fibrosis was measured by positive trichrome staining per mm^2 tissue section, and perivascular fibrosis was measured by identifying 3 to 5 representative vessels per slide, selecting a 0.1mm^2 area centered around the vessel, and exporting the image to ImageJ for analysis of total area of trichrome stain. The ratio of trichrome stain to

total area was calculated, and the results averaged for all representative vessels. Analysis for TUNEL staining was also performed using QuPath software. Three representative 10mm^2 sections were selected per slide, and the QuPath automated detection program was used to detect TUNEL positive and negative nuclei. The ratio of TUNEL positive to negative nuclei was calculated, and the results from the 3 sections averaged.

Immunoblotting

Tissue was lysed in radioimmunoprecipitation assay buffer (Boston Bioproducts, Milford, MA). Ischemic myocardial tissue total protein ($40\mu\text{g}$) was fractionated on a 4% to 12% Bis-Tris gel (ThermoFisher Scientific), transferred to a nitrocellulose or polyvinylidene difluoride membrane (ThermoFisher Scientific, Waltham, MA), and membranes were incubated overnight at 4°C with 1:1000 dilutions of individual rabbit polyclonal primary antibodies to eNOS, phosphorylated (Ser1177) eNOS, Akt, phosphorylated (Ser473) Akt, ERK1/2 (extracellular signal-regulated kinase 1/2), phosphorylated ERK1/2, AMPK, phosphorylated (Thr172) AMPK, superoxide dismutase 2, filamin, α -fodrin, MCP1 (monocyte chemoattractant protein-1),

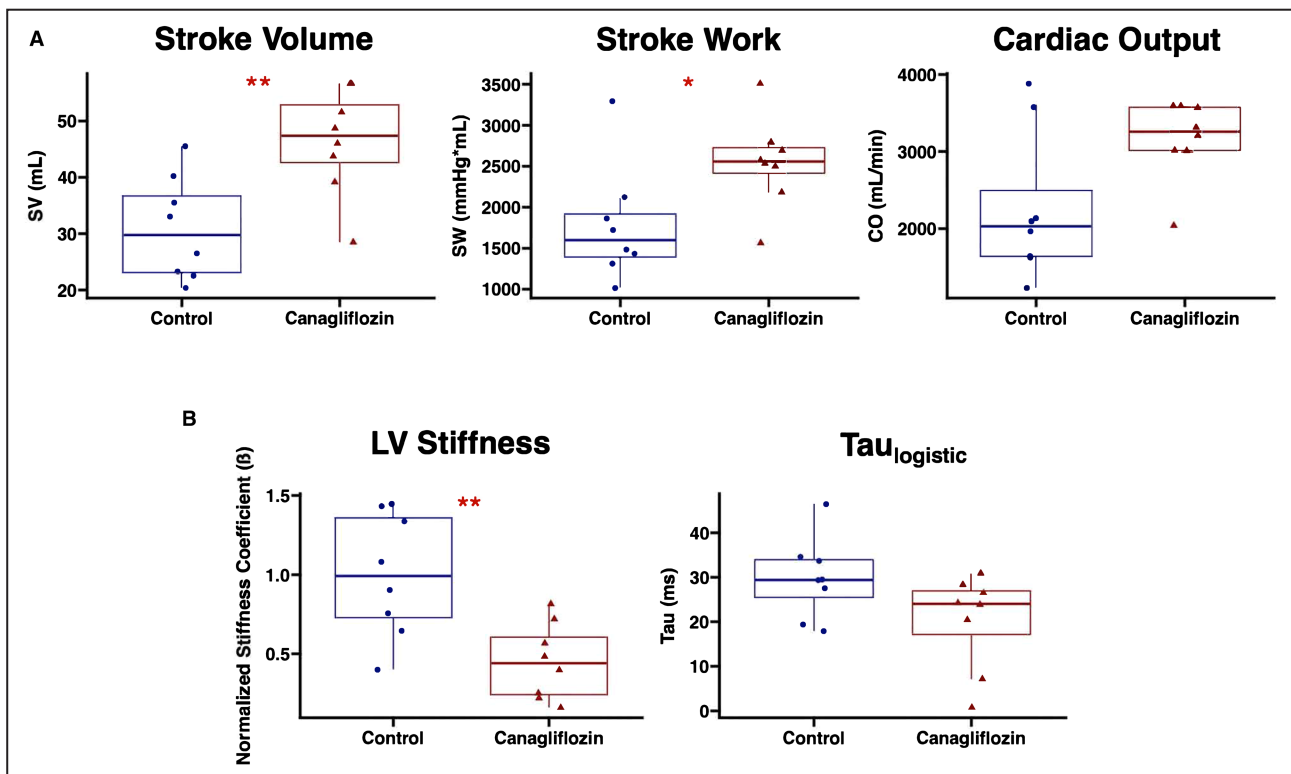


Figure 1. Canagliflozin therapy improves hemodynamic parameters in the setting of chronic myocardial ischemia.

A, Swine treated with canagliflozin ($n=8$) had improved systolic parameters including increased SV and SW compared with control pigs ($n=8$). There was a nonsignificant trend toward increased CO in the canagliflozin-treated pigs compared with controls. **B**, Canagliflozin therapy was also associated with a reduced β as derived from the end-diastolic pressure volume relationship, a marker of LV stiffness. There was a nonsignificant trend toward decreased $\text{tau}_{\text{logistic}}$ in canagliflozin-treated pigs compared with controls. * $P<0.05$. ** $P<0.01$. β indicates stiffness coefficient; CO, cardiac output; LV, left ventricular; SV, stroke volume; and SW, stroke work.

α -actinin, β -actin, desmin, connexin-43, MMP13 (matrix metalloproteinase 13), mTOR (mammalian target of rapamycin), TIMP2 (tissue inhibitor of metalloproteinase 2), troponin T, troponin I, vimentin, jak2, TGF β (transforming growth factor beta), SMAD2/3, STAT3 (signal transducer and activator of transcription 3), phosphorylated STAT3 (Cell Signaling, Danvers, MA), and angiotensin (Abcam, Cambridge, UK). Catalog numbers are listed in Table S1. All membranes were probed with GAPDH (Cell Signaling, Danvers, MA) to correct for loading error. Membranes were incubated with antimouse or antirabbit secondary antibodies (Cell Signaling, Danvers, MA), processed for chemiluminescent detection (Thermo Fisher Scientific, Waltham, MA), and captured with a digital camera system (Bio-Rad ChemiDoc MP, Life Science, Hercules, CA). Densitometric analysis of band intensity was performed using National Institutes of Health ImageJ software. Uncropped blot images provided in Figure S1.

Protein Oxidation Detection

Oxidative stress in ischemic myocardial tissue was determined using an Oxyblot Protein Oxidation Detection Kit (MilliporeSigma, Burlington, MA), which detects carbonyl groups introduced into proteins by oxidative reactions. Tissue was lysed in radioimmunoprecipitation assay buffer (Boston Bioproducts, Milford, MA). A sample of 20 μ g of protein was denatured with 12% sodium dodecyl sulfate,

subjected to 2,4-dinitrophenylhydrazine solution to derivatize the samples, incubated at room temperature for 15 minutes, and neutralized with neutralization solution as per the manufacturer's protocol (MilliporeSigma, Burlington, MA). The samples were fractionated on a 4% to 12% Bis-Tris gel, transferred to a nitrocellulose membrane, incubated with primary and secondary antibodies provided in the kit, processed for chemiluminescent detection, and captured with a digital camera system (Bio-Rad ChemiDoc MP, Life Science, Hercules, CA). Densitometric analysis of total column band intensity was performed using National Institutes of Health ImageJ software.

Statistical Analysis

All data are presented as median value with interquartile ranges. Immunoblot and immunofluorescence data are reported as median fold change values compared with the average control with interquartile ranges. All data were statistically analyzed with Wilcoxon rank-sum test, using R software. Probability values <0.05 were considered significant.

RESULTS

Metabolic Parameters

There were no significant differences in body mass index of animals at the time of ameroid placement or harvest procedure. There were no significant

Table 2. Hemodynamic Parameters

Hemodynamic parameter	Controls	IQR	Canagliflozin	IQR	P value
Heart rate, beats/min	71	63, 77	70	58, 79	0.65
Mean arterial pressure, mmHg	57	53, 63	57	54, 60	1
SV, mL/beat	29.8	23.1, 36.7	47.4	42.6, 52.8	0.007*
SW, mmHg·mL	1599	1392, 1917	2557	2415, 2726	0.02*
Cardiac output, mL/min	2030	1638, 2496	3258	3013, 3574	0.10
dP/dt _{max}	1028.05	828.8, 1066.4	867.2	651.8, 1140.6	0.65
dP/dt _{min}	-1402.8	-1625.1, -1116.0	-1172.5	-2105.6, -948.9	0.80
LVEDP	6.86	4.41, 8.74	7.06	4.48, 8.50	1
LV end-diastolic volume	120.2	113.8, 135.0	118.9	98.3, 151.3	0.96
LV end-systolic pressure	58.1	56.0, 65.7	59.4	55.3, 62.2	0.96
LV end-systolic	97.6	68.6, 104.8	64.5	53.3, 108.1	0.44
Ea, mmHg/mL	1.95	1.61, 2.77	1.21	1.08, 1.63	0.02*
Tau _{logistic} , ms	29.4	25.4, 33.9	24.0	17.1, 26.9	0.10
Slope _{PRSW} , mmHg	41.6	38.3, 43.4	42.1	32.4, 51.5	0.57
X-intercept _{PRSW} , mL	85.4	67.6, 98.0	53.7	48.2, 83.8	0.33
End-systolic elastance, mmHg/mL	1.50	0.86, 3.24	1.27	1.08, 1.99	0.96
Normalized β	0.99	0.73, 1.36	0.44	0.24, 0.61	0.007*

There was a significant increase in SV and SW in canagliflozin-treated pigs (n=8) compared with the control group (n=8). There was a significant decrease in Ea and the left ventricular β as derived from the EDP volume relationship and normalized to average control. dP/dt indicates change in pressure over change in time; Ea, arterial elastance; EDP, end-diastolic pressure; HR, heart rate; IQR interquartile range; LV, left ventricular; PRSW, preload recruitable stroke work relationship; SV, stroke volume; and SW, stroke work.

*P<0.05.

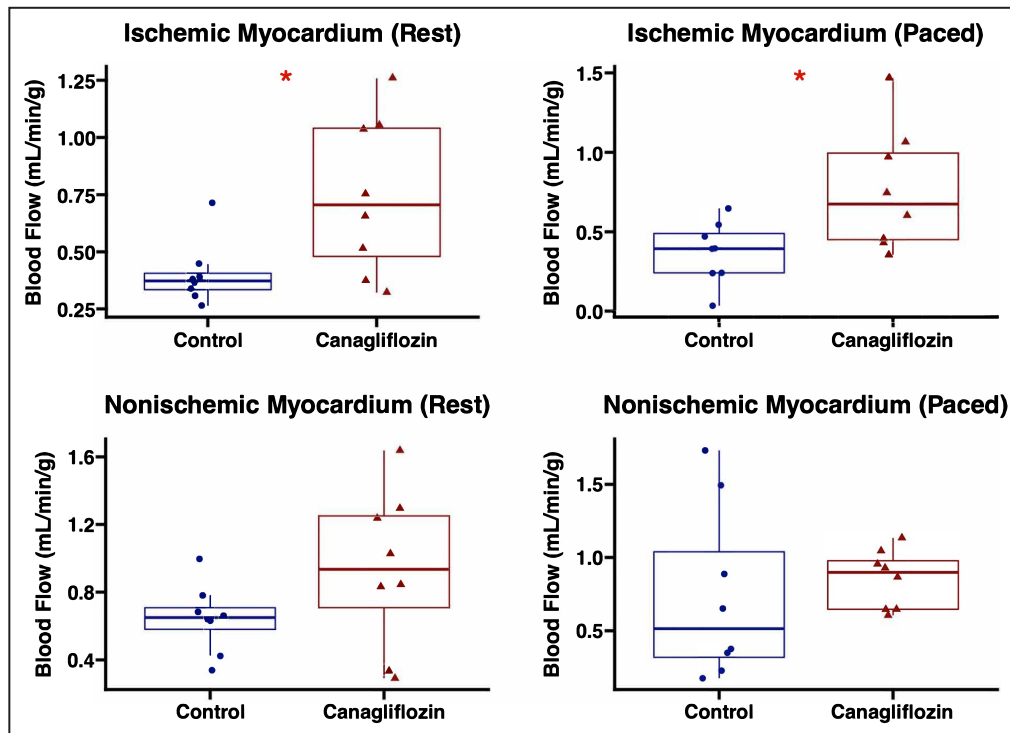


Figure 2. Canagliflozin therapy increases blood flow to ischemic myocardial territory.

Absolute blood flow (mL/min per g) was increased in the ischemic myocardial territory of swine treated with canagliflozin (n=8) compared with controls (n=8). There were no significant differences in absolute blood flow to the nonischemic myocardial territory between groups. * $P < 0.05$.

differences in percent change of body mass index between the ameroid and harvest procedures. There were no differences in baseline glucose or glucose levels at 30 and 60 minutes after dextrose challenge. When compared with the control group, the canagliflozin-treated pigs had increased serum albumin, increased total protein, and increased low-density lipoprotein. There were no significant differences between groups in total bilirubin, direct bilirubin, alkaline phosphatase, alanine aminotransferase, aspartate aminotransferase, total cholesterol, triglycerides, high-density lipoprotein, C-reactive protein, and hemoglobin A1c (Table 1).

Canagliflozin Therapy Improves Systolic and Diastolic Hemodynamic Parameters

There were no significant differences in heart rate between the canagliflozin and control groups.

Load-Dependent Data

Canagliflozin-treated swine had increased stroke volume and stroke work compared with control. There was a nonsignificant trend toward increased cardiac output in the canagliflozin-treated pigs compared with controls. Canagliflozin treatment was also associated with decreased arterial elastance compared with controls.

There was a nonsignificant trend toward decreased tau_{logistic} in the canagliflozin group compared with controls.

Load-Independent Data

There were no significant differences in end-systolic elastance as derived from the end-systolic pressure volume relationship, nor were there differences in the slope or x-intercept of the preload recruitable stroke work equation between groups, all measures of contractility. There was a significant decrease in the normalized left ventricular stiffness coefficient, as derived from the end-diastolic pressure volume relationship, in the canagliflozin group compared with controls (Figure 1, Table 2).

Perfusion to Chronically Ischemic Myocardial Territory Is Increased With Canagliflozin Treatment

Canagliflozin-treated swine had increased absolute blood flow to the ischemic myocardial territory compared with the control group at rest ($P=0.036$) and during pacing to 150 bpm ($P=0.038$). The canagliflozin group had a nonsignificant trend toward increased absolute blood flow to the nonischemic (left anterior descending) territory compared with controls at rest ($P=0.16$). There was no significant difference in absolute blood flow to the nonischemic territory during

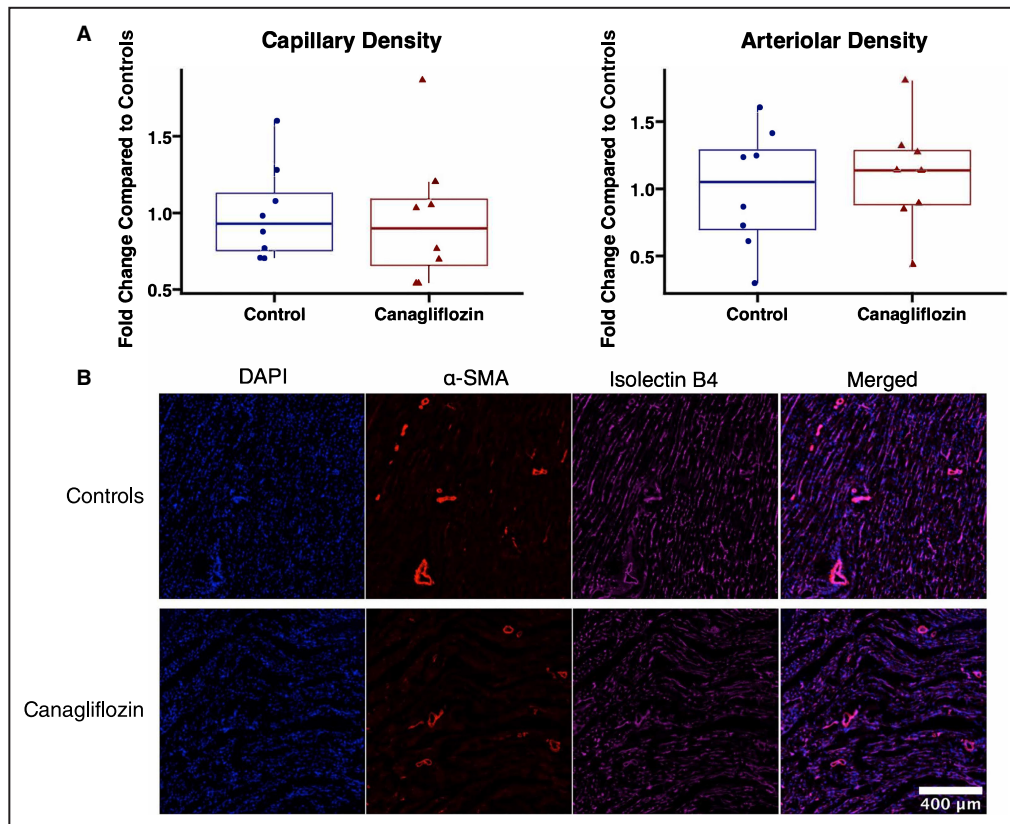


Figure 3. Canagliflozin therapy does not affect microvessel density in chronically ischemic myocardium.

A, In ischemic myocardium, there were no significant differences in capillary density as determined by area of isolectin B4 staining and arteriolar count as determined by α -SMA staining, between canagliflozin-treated pigs ($n=8$) and controls ($n=8$). Capillary and arteriolar density were normalized to the average value in the control group. **B**, Representative images of ischemic myocardial tissue. α -SMA indicates alpha smooth muscle actin.

pace to 150 bpm ($P=0.38$; Figure 2). The proximal circumflex artery in the area of the ameroid constrictor was occluded by visual inspection in all cases.

Coronary Microvascular Density Is Unchanged With Canagliflozin Therapy

There were no significant differences in fold change capillary density, as measured by isolectin B4 immunofluorescence, in ischemic myocardium between groups ($P=0.57$). There were no significant differences in fold change arteriolar count between groups

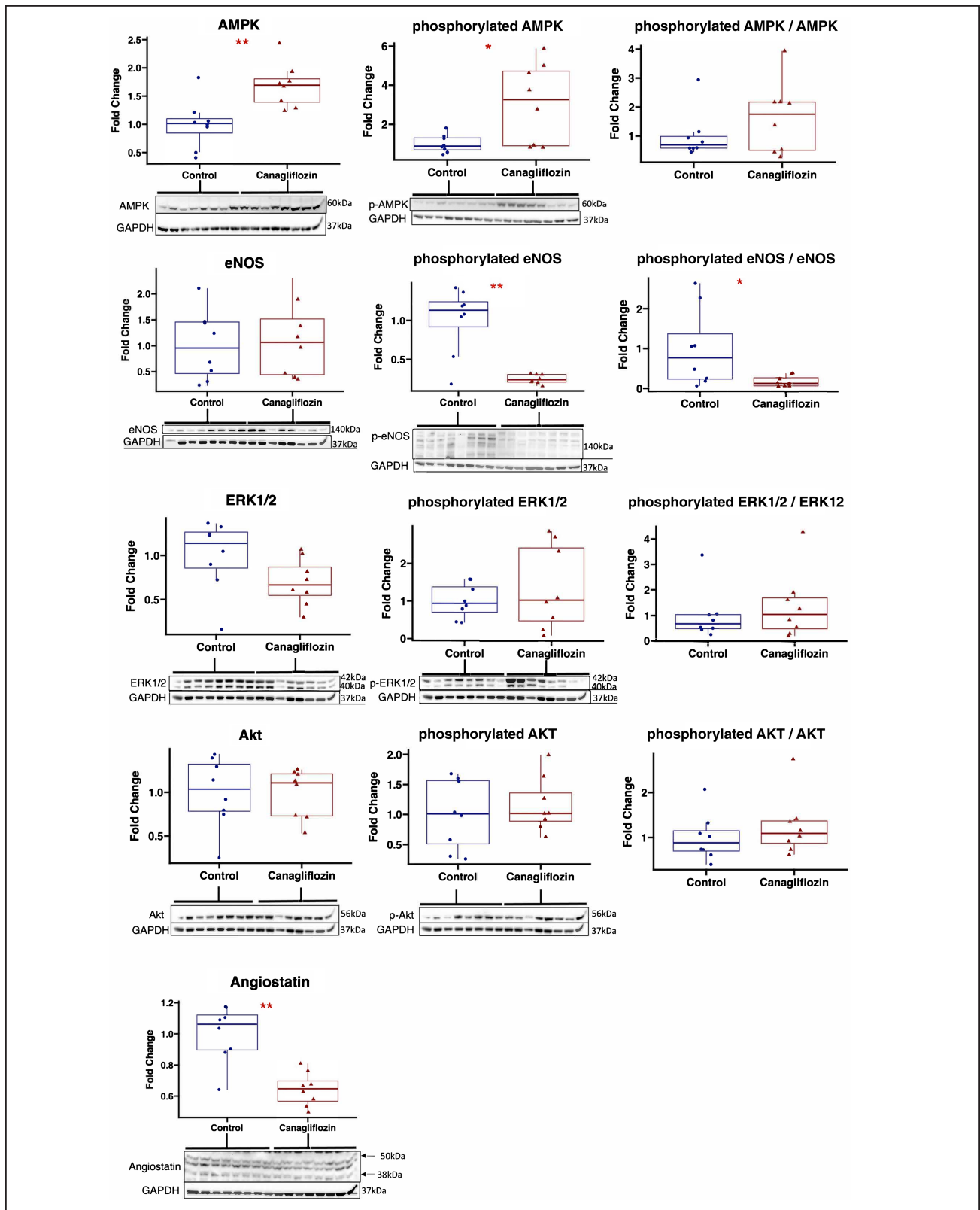
($P=0.72$), as determined by α -SMA immunofluorescence in ischemic myocardium (Figure 3).

Canagliflozin Has Mixed Effects on Angiogenic Signaling Pathways in Chronically Ischemic Myocardium

In ischemic myocardium of the canagliflozin-treated pigs, immunoblot experiments showed increased expression of total AMPK ($P=0.0047$) and phosphorylated AMPK ($P=0.038$) compared with controls, with no change in the phosphorylated AMPK to AMPK ratio

Figure 4. Effect of canagliflozin on angiogenic signaling pathways in chronically ischemic myocardium.

Chronically ischemic myocardium in swine treated with canagliflozin ($n=8$) had increased expression of total AMPK and phosphorylated AMPK compared with controls ($n=8$). There was a trend toward decreased total ERK1/2 expression with canagliflozin therapy compared with controls, without changes in phosphorylated ERK1/2 expression. Total eNOS expression was unchanged between groups, but there was decreased expression of phosphorylated eNOS in the canagliflozin-treated group compared with controls. Canagliflozin therapy was also associated with decreased expression of angiotensin (bands at 38 kDa and 50 kDa quantitated). Values expressed as fold change compared with average value in control group. Upper and lower borders of box represent upper and lower quartiles, middle horizontal line represents median, upper and lower whiskers represent maximum and minimum values. * $P<0.05$, ** $P<0.01$. AMPK indicates 5' adenosine monophosphate-activated protein kinase; eNOS, endothelial nitric oxide synthase; and ERK1/2, extracellular signal-regulated kinase 1/2.



($P=0.57$). Total eNOS expression was unchanged between groups ($P=0.88$), though the canagliflozin group had decreased expression of phosphorylated eNOS ($P=0.007$), with a decrease in the phosphorylated

eNOS to eNOS ratio ($P=0.028$). There was a trend toward decreased total ERK1/2 expression in the canagliflozin group ($P=0.08$), without changes in phosphorylated ERK1/2 ($P=0.80$) or the phosphorylated

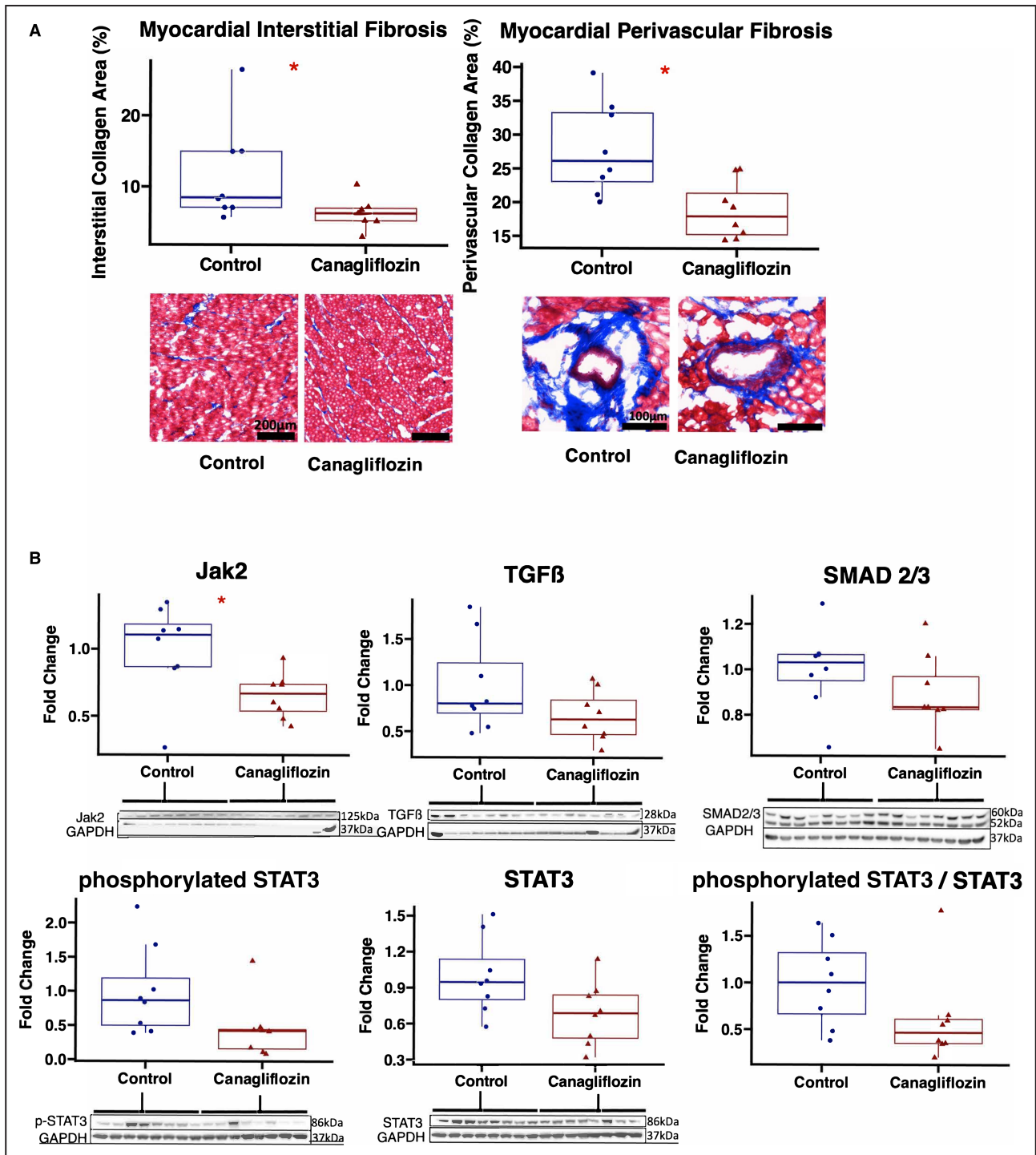


Figure 5. Canagliflozin therapy reduces myocardial interstitial and perivascular fibrosis in chronically ischemic myocardium with decreased Jak/STAT signaling.

A, Representative images of ischemic myocardial tissue with trichrome staining (20x magnification). Quantitative analyses of interstitial and perivascular fibrosis were carried out using QuPath software. Values expressed as fold change compared with average value in control group. **B**, Chronically ischemic myocardium in swine treated with canagliflozin (n=8) had decreased expression of Jak2, with strong trends toward decreased phosphorylated STAT3, and the ratio of phosphorylated STAT3/STAT3 compared with controls. There were nonsignificant trends toward decreased expression of STAT3, TGFβ, and SMAD2/3 in canagliflozin-treated swine compared with controls (n=8). Values expressed as fold change compared with average value in control group. Upper and lower borders of box represent upper and lower quartiles, middle horizontal line represents median, upper and lower whiskers represent maximum and minimum values. *P<0.05, **P<0.01. Jak2 indicates Janus kinase 2; STAT3, signal transducer and activator of transcription 3; and TGFβ, transforming growth factor beta.

Table 3. Fibrotic Protein Expression

Protein	Controls	IQR	Canagliflozin	IQR	P value
α -fodrin	0.92	0.86, 1.02	0.78	0.65, 0.84	0.015*
α -actinin	1.06	0.87, 1.15	0.75	0.72, 0.83	0.10
β -actin	0.85	0.49, 1.00	0.28	0.26, 0.30	0.08*
Connexin-43	0.96	0.93, 1.09	0.66	0.59, 0.90	0.014*
Desmin	0.45	0.34, 0.54	0.68	0.53, 0.89	0.09
Filamin	0.99	0.91, 1.1	1.06	0.91, 1.28	0.51
MCP-1	1.03	0.81, 1.14	0.47	0.29, 0.73	0.028*
MMP13	1.0	0.89, 1.24	0.76	0.70, 0.77	0.021*
mTOR	0.94	0.60, 1.45	0.79	0.61, 0.94	0.57
TIMP2	1.1	0.64, 1.21	0.27	0.23, 0.41	0.002*
Troponin I	0.98	0.91, 1.20	0.67	0.63, 0.82	0.007*
Troponin T	0.85	0.81, 1.30	0.77	0.66, 0.94	0.16
Vimentin	1.04	0.56, 1.45	0.23	0.19, 0.33	0.07

Canagliflozin-treated (n=8) swine had decreased expression of α -fodrin, β -actin, connexin-43, MCP-1, MMP13, TIMP2, and troponin I compared with control (n=8). There were no significant differences in expression of α -actinin, desmin, filamin, mTOR, troponin T, and vimentin. Values expressed as fold change compared with average value in control group.

IQR indicates interquartile range; MCP-1, monocyte chemoattractant protein 1; MMP13, matrix metalloproteinase 13; and mTOR, mammalian target of rapamycin.

* $P < 0.05$.

ERK1/2 to ERK1/2 ratio ($P=0.51$). There was decreased expression of angiotensin II in the canagliflozin group compared with controls ($P=0.002$). There were no significant differences in expression of total Akt ($P=0.57$), phosphorylated Akt ($P=0.65$), or the phosphorylated AKT to AKT ratio ($P=0.33$) between groups (Figure 4).

Canagliflozin Reduces Fibrosis and Profibrotic Molecular Signaling in Chronically Ischemic Myocardium

Canagliflozin therapy was associated with decreased interstitial fibrosis ($P=0.04$) and decreased perivascular fibrosis ($P=0.010$) in ischemic myocardium compared with controls as measured by collagen trichrome staining (Figure 5, 1 outlier excluded from interstitial fibrosis analysis as tissue section had abnormally high amount of trichrome staining not typical in this model). Immunoblot experiments of fibrotic markers in ischemic myocardium showed decreased Jak/STAT signaling as indicated by decreased expression of Jak2 ($P=0.021$), and a strong trend toward decreased expression of phosphorylated STAT3 ($P=0.065$), and the ratio of phosphorylated STAT3/STAT3 ($P=0.065$). There was a nonsignificant trend toward decreased expression of TGF β ($P=0.16$) and SMAD2/3 ($P=0.16$) in the canagliflozin group compared with controls (Figure 5). The canagliflozin group had decreased expression of MCP-1, MMP13, TIMP2, and structural proteins α -fodrin, connexin-43, and troponin I compared with controls, with a trend toward decreased α -actinin, β -actin, vimentin, and troponin T expression. There was a trend toward increased expression of desmin in

the canagliflozin group compared with controls, but no significant differences in expression of mTOR or filamin between groups (Table 3, Figure S2).

Canagliflozin Reduces Total Protein Oxidation and Increases Antioxidant Signaling in Chronically Ischemic Myocardium

Total protein oxidation as determined by Oxyblot staining was significantly decreased in the canagliflozin-treated pigs compared with controls ($P=0.014$). There was increased expression of mitochondrial antioxidant superoxide dismutase 2 in the canagliflozin group compared with controls ($P < 0.001$; Figure 6).

Apoptosis in Chronically Ischemic Myocardium Is Unchanged in Swine Treated With Canagliflozin

There were no significant differences between groups in apoptosis in ischemic myocardial tissue as measured by TUNEL staining ($P=0.72$; Figure S3).

DISCUSSION

In the present study, we found that in our large animal model of chronic myocardial ischemia, canagliflozin therapy, when compared with vehicle treatment, is associated with (1) improved hemodynamic function including increased stroke volume, increased stroke work, and reduced left ventricular stiffness; (2) improved perfusion to ischemic myocardial territory; (3)

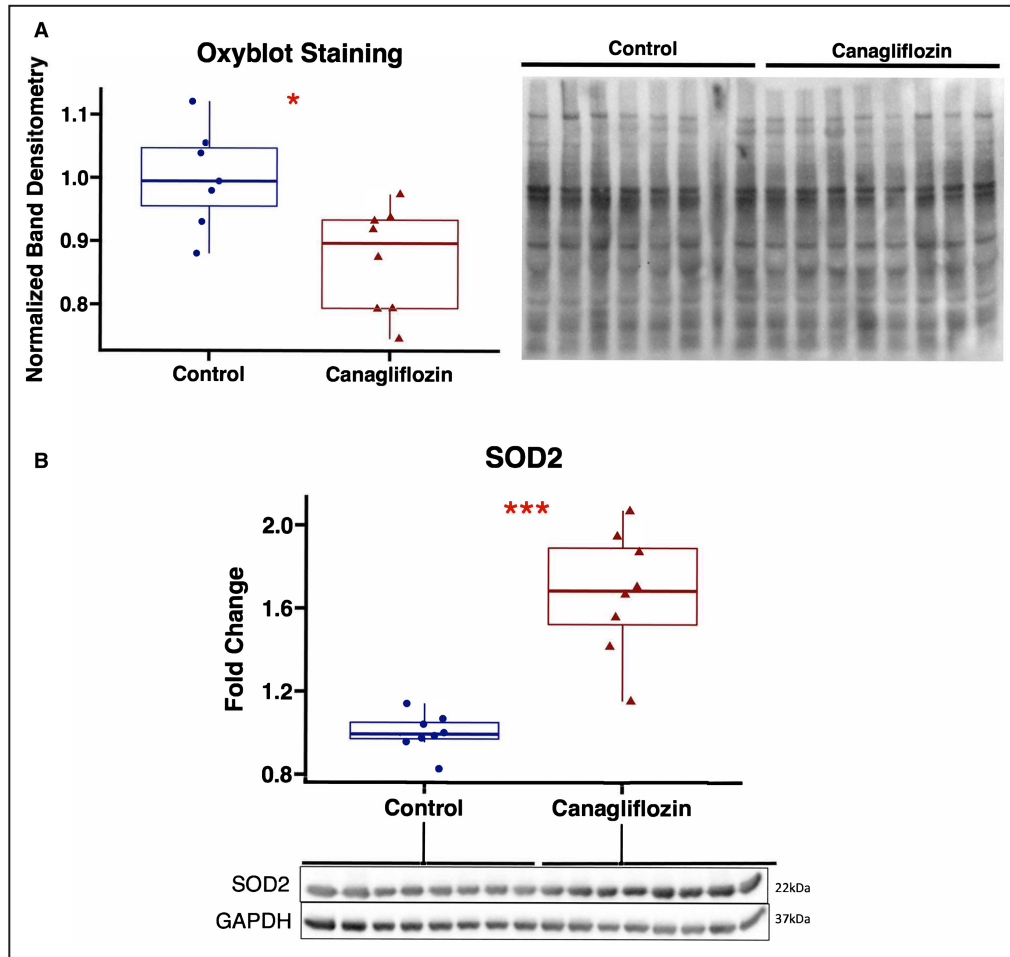


Figure 6. Canagliflozin therapy decreases oxidative stress in chronically ischemic myocardium.

A, Protein oxidation as measured by Oxyblot staining was decreased in canagliflozin-treated pigs (n=8) compared with controls (n=7, 1 sample excluded owing to poor sample run on gel). Band densitometry of entire lane for each sample normalized to average value in control group. **B**, Expression of mitochondrial antioxidant SOD2 was significantly increased in canagliflozin-treated pigs compared with controls. Upper and lower borders of box represent upper and lower quartiles, middle horizontal line represents median, upper and lower whiskers represent maximum and minimum values. * $P < 0.05$. SOD2 indicates superoxide dismutase 2.

no change in capillary or arteriolar density in ischemic myocardial tissue; (4) increased expression and activation of AMPK; (5) reduced interstitial and perivascular fibrosis with concomitant downregulation of Jak/STAT signaling; and (6) reduced oxidative stress in ischemic myocardium. Taken together, these findings provide novel evidence of the functional and molecular effects of canagliflozin in chronically ischemic myocardium.

The effect of canagliflozin therapy on hemodynamic function has previously been investigated in animal models of acute ischemia.^{4,24} In a rat study of acute canagliflozin treatment in nondiabetic rats with ischemia/reperfusion injury, acute intravenous canagliflozin therapy improved left ventricular contractility and diastolic function.⁵ Baker et al investigated the effects of canagliflozin in a swine model of acute ischemia/reperfusion injury to the LCx territory and found that

acute canagliflozin therapy improved stroke volume and stroke work.⁴ In another swine model of temporary left anterior descending coronary artery occlusion-induced heart failure, empagliflozin, another SGLT2i, improved diastolic function 2 months after ischemic insult; authors noted reduced cardiomyocyte stiffness and fibrosis, which possibly contributed to these effects.²⁴ These studies demonstrated the beneficial effect of SGLT2i on myocardial function after acute ischemic insult. To our knowledge, the present study is the first large animal study that demonstrates improved hemodynamic function with canagliflozin therapy in the setting of chronic myocardial ischemia in a large animal model, a model more similar to what patients with diabetes or heart failure may experience. Additionally, we found that canagliflozin therapy was associated with reduced left ventricular stiffness, which can be one of the earliest

abnormalities in progression to congestive heart failure.²⁵ This finding is of particular interest given the clinical benefit that SGLT2is have in patients with heart failure with preserved ejection fraction. Reduced stiffness in our model is likely secondary in part to reduced interstitial fibrosis, a significant finding in the context of chronic myocardial ischemia that may be clinically relevant in patients with chronic coronary disease who subsequently develop ischemic cardiomyopathy.

Additionally, we found that in our model of chronic myocardial ischemia, canagliflozin therapy improved myocardial perfusion to the ischemic territory. Previous animal models of acute myocardial ischemia have not demonstrated an effect of SGLT2is on myocardial perfusion,^{3,4} which may suggest duration-dependent effects of SGLT2 inhibition. Interestingly, in the current study, the increased blood flow was not accompanied by increased microvessel collateralization, including capillary and arteriolar formation. One plausible mechanism for improved perfusion with canagliflozin therapy may be, as reported in this study, reduced perivascular fibrosis. Further, improved endothelium-dependent or independent vasodilation may account for improved myocardial perfusion. Canagliflozin has been previously shown to improve coronary vasodilation,^{26,27} though determination of endothelium-dependent and independent effects have been better investigated in other vascular beds.²⁸ Although canagliflozin treatment was associated with a decrease in phosphorylated eNOS at the activating Ser1177 site, reduced oxidative stress as demonstrated by Oxyblot staining may improve nitric oxide bioavailability and eNOS coupling, thereby improving endothelium-dependent vasodilation. Additionally, increased myocardial perfusion in the canagliflozin group could be in part secondary to decreased expression of angiotensin, which in addition to its antiangiogenic activity is also a negative regulator of endothelium-dependent vasodilation.²⁹ Microvascular reactivity studies may be warranted to definitively evaluate the effect of canagliflozin on coronary vasomotor tone in the setting of chronic myocardial ischemia.

In addition to evaluating myocardial function and perfusion in response to canagliflozin therapy, we sought to evaluate several molecular pathways to determine how canagliflozin exerts beneficial effects on chronically ischemic myocardium. With regard to fibrotic signaling, we found that canagliflozin therapy downregulated the profibrotic Jak/STAT signaling pathway, which is a key promoter of fibroblast activation and ischemia-induced cardiac dysfunction.^{30,31} These findings were supported by reduced expression of MCP-1, a profibrotic cytokine that is transcriptionally upregulated by Jak/STAT signaling.³² This study is the first, to our knowledge, to investigate canagliflozin-induced reduction of Jak/STAT/MCP-1 signaling. Additionally, canagliflozin therapy was associated with reduced expression of

TIMP2, β -actin, connexin-43, troponin I, and MMP13, with trends toward decreased TGF β and SMAD2/3, all of which have been associated with increased fibrosis.^{33–37} Consistent with other models investigating the effects of SGLT2i in myocardium,^{7,38} we found increased myocardial expression of total and activated AMPK in canagliflozin-treated swine. AMPK activation has been an area of interest in the treatment of heart disease, as it is involved in regulation of several important processes, including cardiac metabolism, gene transcription, mitochondrial function, apoptosis, and autophagy.³⁹ Further investigation into these pathways may provide additional insight into the mechanisms by which SGLT2is affect ischemic myocardium. We also investigated expression and activation of proangiogenic signaling markers, including ERK1/2, Akt, and eNOS, with canagliflozin treatment in our model. There were no changes in total or activated forms of Akt, activated ERK1/2, or total eNOS, but there was reduced expression of total ERK1/2, and surprisingly, canagliflozin therapy was associated with decreased phosphorylation/activation of eNOS in our model, contrary to findings in other animal models of myocardial injury with SGLT2i therapy.^{5,40} Perhaps canagliflozin has differential effects on eNOS activation in the setting of acute and chronic ischemia, or duration-dependent temporal effects may play a role. Importantly, canagliflozin therapy was associated with decreased oxidative stress in chronically ischemic myocardium, an effect that may be mediated by increased expression of the endogenous mitochondrial antioxidant superoxide dismutase 2. Further studies are necessary to investigate the detailed molecular pathways affected by canagliflozin therapy.

Canagliflozin therapy did not significantly affect most of the metabolic parameters assessed in this study, including body mass index and glucose tolerance testing. The pigs in this model received a normal diet and we did not expect to see any significant difference in glucose tolerance testing in this cohort. Interestingly, serum albumin, total protein, and low-density lipoprotein levels were increased in the canagliflozin-treated pigs, whereas there was a trend toward decreased triglyceride levels with treatment. The effects of SGLT2is on low-density lipoprotein and triglycerides are documented in the literature and may be secondary to reduced low-density lipoprotein clearance and increased lipolysis of triglyceride-rich lipoproteins.⁴¹ Canagliflozin is known to decrease albuminuria, specifically in the context of chronic kidney disease,¹⁰ and though these effects would not be expected to be dramatic in this cohort of otherwise healthy pigs, perhaps a small reduction in urinary albumin losses would account for the minimal increases in serum albumin and total protein with treatment.

The beneficial effects of canagliflozin therapy in this model of chronic myocardial ischemia provide insight into functional and molecular mechanisms by which

SGLT2is may improve clinical outcomes in patients with cardiovascular disease. Indications for SGLT2is have broadened to include patients with heart failure with preserved ejection fraction and symptomatic heart failure with reduced ejection fraction,¹⁵ and the findings in this study support further investigation into the role of SGLT2is specifically in the setting of chronic coronary artery disease. The results of ongoing clinical trials on the effects of SGLT2is on acute myocardial ischemia will be informative.¹⁷ In addition to canagliflozin, other SGLT2is commonly investigated include empagliflozin and dapagliflozin, and these agents may have differential effects.⁴² It may be interesting to study the differential effects of these 3 SGLT2is in the setting of chronic myocardial ischemia.

Study Limitations

There are several limitations in this study to consider. As previously discussed, the increased perfusion but lack of capillary or arteriolar collateralization warrant microvascular reactivity studies. Future studies using microvascular reactivity will help define whether canagliflozin treatment augments endothelium-dependent or -independent vasodilation or extravascular factors. Further, our functional, perfusion, and molecular data capture only a single time point 5 weeks after initiation of canagliflozin therapy, and as previously discussed it may be informative to investigate whether there are differential effects of short- versus long-term treatment. Additionally, given the large animal model, we have a relatively small sample size of 8 animals per group, and there were several trends that approached significance that may have been unmasked by a larger sample size. An additional statistical limitation in this study is the large number of statistical comparisons we performed, some that could be statistically significant owing to chance alone. Finally, in investigating the molecular effects of canagliflozin in chronically ischemic myocardium, we investigated several key molecular pathways, but there are likely other important contributing mechanisms that are still unknown. Future studies focusing on proteomic and transcriptomic analyses will help further delve into the molecular alterations that occur with canagliflozin therapy in the setting of chronic myocardial ischemia in order to better understand these mechanisms.

CONCLUSIONS

In summary, canagliflozin therapy in the setting of chronic myocardial ischemia improves myocardial function and perfusion to ischemic myocardium, without affecting microvascular collateralization. Reduced interstitial and perivascular fibrosis via inhibition of Jak/STAT signaling, activation of AMPK, and antioxidant signaling may contribute to these effects. Given the

promising results of this study among others, further investigation into the role of SGLT2is as a therapeutic agent for chronic coronary artery disease may be warranted.

ARTICLE INFORMATION

Received October 26, 2022; accepted November 28, 2022.

Affiliation

Division of Cardiothoracic Surgery, Department of Surgery, Cardiovascular Research Center, Rhode Island Hospital, Alpert Medical School of Brown University, Rhode Island Hospital, Providence, RI.

Acknowledgments

We thank the veterinary and animal care staff at Rhode Island Hospital for their excellent care of the animals used in this study.

Sources of Funding

Funding for this research was provided by the National Heart, Lung, and Blood Institute 1F32HL160063-01 (S.A.S.); T32GM065085-10 (C.M.X.); NIHT32HL160517 (D.D.H.); 1R01HL133624 (M.R.A.); 2R56HL133624-05 (M.R.A.); R01HL46716 and R01HL128831 (F.W.S.).

Disclosures

None.

Supplemental Material

Table S1
Figures S1–S3

REFERENCES

- Lassaletta AD, Chu LM, Sellke FW. Therapeutic neovascularization for coronary disease: current state and future prospects. *Basic Res Cardiol*. 2011;106:897–909. doi: [10.1007/s00395-011-0200-1](https://doi.org/10.1007/s00395-011-0200-1)
- Knuuti J, Wijns W, Saraste A, Capodanno D, Barbato E, Funck-Brentano C, Prescott E, Storey RF, Deaton C, Cuisset T, et al. 2019 ESC guidelines for the diagnosis and management of chronic coronary syndromes. *Eur Heart J*. 2020;41:407–477. doi: [10.1093/eurheartj/ehz425](https://doi.org/10.1093/eurheartj/ehz425)
- Lim VG, Bell RM, Arjun S, Kolatsi-Joannou M, Long DA, Yellon DM. SGLT2 inhibitor, canagliflozin, attenuates myocardial infarction in the diabetic and nondiabetic heart. *JACC Basic Transl Sci*. 2019;4:15–26. doi: [10.1016/j.jacbs.2018.10.002](https://doi.org/10.1016/j.jacbs.2018.10.002)
- Baker HE, Kiel AM, Luebbe ST, Simon BR, Earl CC, Regmi A, Roell WC, Mather KJ, Tune JD, Goodwill AG. Inhibition of sodium–glucose cotransporter-2 preserves cardiac function during regional myocardial ischemia independent of alterations in myocardial substrate utilization. *Basic Res Cardiol*. 2019;114:25. doi: [10.1007/s00395-019-0733-2](https://doi.org/10.1007/s00395-019-0733-2)
- Sayour AA, Korkmaz-Icöz S, Loganathan S, Ruppert M, Sayour VN, Oláh A, Benke K, Brune M, Benkő R, Horváth EM, et al. Acute canagliflozin treatment protects against in vivo myocardial ischemia–reperfusion injury in non-diabetic male rats and enhances endothelium-dependent vasorelaxation. *J Transl Med*. 2019;17:127. doi: [10.1186/s12967-019-1881-8](https://doi.org/10.1186/s12967-019-1881-8)
- Tsai K-F, Chen Y-L, Chiou TT-Y, Chu T-H, Li L-C, Ng H-Y, Lee W-C, Lee C-T. Emergence of SGLT2 inhibitors as powerful antioxidants in human diseases. *Antioxidants (Basel)*. 2021;10:1166. doi: [10.3390/antiox10081166](https://doi.org/10.3390/antiox10081166)
- Kondo H, Akoumianakis I, Badi I, Akawi N, Kotanidis CP, Polkinghorne M, Stadiotti I, Sommariva E, Antonopoulos AS, Carena MC, et al. Effects of canagliflozin on human myocardial redox signalling: clinical implications. *Eur Heart J*. 2021;42:4947–4960. doi: [10.1093/eurheartj/ehab420](https://doi.org/10.1093/eurheartj/ehab420)
- Wiviott SD, Raz I, Bonaca MP, Mosenzon O, Kato ET, Cahn A, Silverman MG, Zelniker TA, Kuder JF, Murphy SA, et al. Dapagliflozin and cardiovascular outcomes in type 2 diabetes. *N Engl J Med*. 2019;380:347–357. doi: [10.1056/NEJMoa1812389](https://doi.org/10.1056/NEJMoa1812389)
- Zinman B, Wanner C, Lachin JM, Fitchett D, Bluhmki E, Hantel S, Mattheus M, Devins T, Johansen OE, Woerle HJ, et al. Empagliflozin, cardiovascular outcomes, and mortality in type 2 diabetes. *N Engl J Med*. 2015;373:2117–2128. doi: [10.1056/NEJMoa1504720](https://doi.org/10.1056/NEJMoa1504720)

10. Perkovic V, Jardine MJ, Neal B, Bompoint S, Heerspink HJL, Charytan DM, Edwards R, Agarwal R, Bakris G, Bull S, et al. Canagliflozin and renal outcomes in type 2 diabetes and nephropathy. *N Engl J Med*. 2019;380:2295–2306. doi: [10.1056/NEJMoa1811744](https://doi.org/10.1056/NEJMoa1811744)
11. Inzucchi SE, Kosiborod M, Fitchett D, Wanner C, Hehne U, Kaspers S, George JT, Zinman B. Improvement in cardiovascular outcomes with empagliflozin is independent of glycemic control. *Circulation*. 2018;138:1904–1907. doi: [10.1161/CIRCULATIONAHA.118.035759](https://doi.org/10.1161/CIRCULATIONAHA.118.035759)
12. Anker SD, Butler J, Filippatos G, Ferreira JP, Bocchi E, Böhm M, Brunner-La Rocca H-P, Choi D-J, Chopra V, Chuquiure-Valenzuela E, et al. Empagliflozin in heart failure with a preserved ejection fraction. *N Engl J Med*. 2021;385:1451–1461. doi: [10.1056/NEJMoa2107038](https://doi.org/10.1056/NEJMoa2107038)
13. McMurray JJV, Solomon SD, Inzucchi SE, Køber L, Kosiborod MN, Martinez FA, Ponikowski P, Sabatine MS, Anand IS, Bělohávek J, et al. Dapagliflozin in patients with heart failure and reduced ejection fraction. *N Engl J Med*. 2019;381:1995–2008. doi: [10.1056/NEJMoa1911303](https://doi.org/10.1056/NEJMoa1911303)
14. Packer M, Anker SD, Butler J, Filippatos G, Pocock SJ, Carson P, Januzzi J, Verma S, Tsutsui H, Brueckmann M, et al. Cardiovascular and renal outcomes with empagliflozin in heart failure. *N Engl J Med*. 2020;383:1413–1424. doi: [10.1056/NEJMoa2022190](https://doi.org/10.1056/NEJMoa2022190)
15. Heidenreich PA, Bozkurt B, Aguilar D, Allen LA, Byun JJ, Colvin MM, Deswal A, Drazner MH, Dunlay SM, Evers LR, et al. 2022 AHA/ACC/HFSA guideline for the management of heart failure: a report of the American College of Cardiology/American Heart Association Joint Committee on Clinical Practice Guidelines. *Circulation*. 2022;145:e895–e1032. doi: [10.1161/CIR.0000000000001063](https://doi.org/10.1161/CIR.0000000000001063)
16. Verma S, Mazer CD, Yan AT, Mason T, Garg V, Teoh H, Zuo F, Quan A, Farkouh ME, Fitchett DH, et al. Effect of empagliflozin on left ventricular mass in patients with type 2 diabetes mellitus and coronary artery disease: the EMPA-HEART CardioLink-6 randomized clinical trial. *Circulation*. 2019;140:1693–1702. doi: [10.1161/CIRCULATIONAHA.119.042375](https://doi.org/10.1161/CIRCULATIONAHA.119.042375)
17. Udell JA, Jones WS, Petrie MC, Harrington J, Anker SD, Bhatt DL, Hernandez AF, Butler J. Sodium glucose cotransporter-2 inhibition for acute myocardial infarction: JACC review topic of the week. *J Am Coll Cardiol*. 2022;79:2058–2068. doi: [10.1016/j.jacc.2022.03.353](https://doi.org/10.1016/j.jacc.2022.03.353)
18. Potz BA, Scrimgeour LA, Pavlov VI, Sodha NR, Abid MR, Sellke FW. Extracellular vesicle injection improves myocardial function and increases angiogenesis in a swine model of chronic ischemia. *J Am Heart Assoc*. 2018;7:7. doi: [10.1161/JAHA.117.008344](https://doi.org/10.1161/JAHA.117.008344)
19. Scrimgeour LA, Potz BA, Aboul Gheit A, Shi G, Stanley M, Zhang Z, Sodha NR, Ahsan N, Abid MR, Sellke FW. Extracellular vesicles promote arteriogenesis in chronically ischemic myocardium in the setting of metabolic syndrome. *J Am Heart Assoc*. 2019;8(15):e012617. doi: [10.1161/JAHA.119.012617](https://doi.org/10.1161/JAHA.119.012617)
20. Aboulgheit A, Karbasiashfar C, Zhang Z, Sabra M, Shi G, Tucker A, Sodha N, Abid MR, Sellke FW. Lactobacillus plantarum probiotic induces Nrf2-mediated antioxidant signaling and eNOS expression resulting in improvement of myocardial diastolic function. *Am J Physiol Heart Circ Physiol*. 2021;321:H839–H849. doi: [10.1152/ajpheart.00278.2021](https://doi.org/10.1152/ajpheart.00278.2021)
21. White FC, Carroll SM, Magnet A, Bloor CM. Coronary collateral development in swine after coronary artery occlusion. *Circ Res*. 1992;71:1490–1500. doi: [10.1161/01.RES.71.6.1490](https://doi.org/10.1161/01.RES.71.6.1490)
22. Elmadhun NY, Lassaletta AD, Chu LM, Liu YJF, Sellke FW. Atorvastatin increases oxidative stress and modulates angiogenesis in Ossabaw swine with the metabolic syndrome. *J Thorac Cardiovasc Surg*. 2012;144:1486–1493. doi: [10.1016/j.jtcvs.2012.08.065](https://doi.org/10.1016/j.jtcvs.2012.08.065)
23. Bankhead P, Loughrey MB, Fernández JA, Dombrowski Y, McArt DG, Dunne PD, McQuaid S, Gray RT, Murray LJ, Coleman HG, et al. QuPath: open source software for digital pathology image analysis. *Sci Rep*. 2017;7:16878. doi: [10.1038/s41598-017-17204-5](https://doi.org/10.1038/s41598-017-17204-5)
24. Santos-Gallego CG, Requena-Ibanez JA, San Antonio R, Garcia-Ropero A, Ishikawa K, Watanabe S, Picatoste B, Vargas-Delgado AP, Flores-Umanzor EJ, Sanz J, et al. Empagliflozin ameliorates diastolic dysfunction and left ventricular fibrosis/stiffness in nondiabetic heart failure: a multimodality study. *JACC Cardiovasc Imaging*. 2021;14:393–407. doi: [10.1016/j.jcmg.2020.07.042](https://doi.org/10.1016/j.jcmg.2020.07.042)
25. Ishikawa K, Agüero J, Oh JG, Hammoudi N, Fish LA, Leonardson L, Picatoste B, Santos-Gallego CG, Fish KM, Hajjar RJ. Increased stiffness is the major early abnormality in a pig model of severe aortic stenosis and predisposes to congestive heart failure in the absence of systolic dysfunction. *J Am Heart Assoc*. 2015;4:e001925. doi: [10.1161/JAHA.115.001925](https://doi.org/10.1161/JAHA.115.001925)
26. Uthman L, Baartscheer A, Bleijlevens B, Schumacher CA, Fiolet JWT, Koeman A, Jancev M, Hollmann MW, Weber NC, Coronel R, et al. Class effects of SGLT2 inhibitors in mouse cardiomyocytes and hearts: inhibition of Na⁺/H⁺ exchanger, lowering of cytosolic Na⁺ and vasodilation. *Diabetologia*. 2018;61:722–726. doi: [10.1007/s00125-017-4509-7](https://doi.org/10.1007/s00125-017-4509-7)
27. Han Y, Cho Y-E, Ayon R, Guo R, Youssef KD, Pan M, Dai A, Yuan JX-J, Makino A. SGLT inhibitors attenuate NO-dependent vascular relaxation in the pulmonary artery but not in the coronary artery. *Am J Physiol Lung Cell Mol Physiol*. 2015;309:L1027–L1036. doi: [10.1152/ajplung.00167.2015](https://doi.org/10.1152/ajplung.00167.2015)
28. Durante W, Behnammanesh G, Peyton KJ. Effects of sodium-glucose co-transporter 2 inhibitors on vascular cell function and arterial remodeling. *Int J Mol Sci*. 2021;22:8786. doi: [10.3390/ijms22168786](https://doi.org/10.3390/ijms22168786)
29. Koshida R, Ou J, Matsunaga T, Chilian WM, Oldham KT, Ackerman AW, Pritchard KA. Angiotensin: a negative regulator of endothelial-dependent vasodilation. *Circulation*. 2003;107:803–806. doi: [10.1161/01.CIR.0000057551.88851.09](https://doi.org/10.1161/01.CIR.0000057551.88851.09)
30. Mascareno E, El-Shafei M, Maulik N, Sato M, Guo Y, Das DK, Siddiqui MA. JAK/STAT signaling is associated with cardiac dysfunction during ischemia and reperfusion. *Circulation*. 2001;104:325–329. doi: [10.1161/01.CIR.104.3.325](https://doi.org/10.1161/01.CIR.104.3.325)
31. Chakraborty D, Šumová B, Mallano T, Chen C-W, Distler A, Bergmann C, Ludolph I, Horch RE, Gelse K, Ramming A, et al. Activation of STAT3 integrates common profibrotic pathways to promote fibroblast activation and tissue fibrosis. *Nat Commun*. 2017;8:1130. doi: [10.1038/s41467-017-01236-6](https://doi.org/10.1038/s41467-017-01236-6)
32. Potula HSK, Wang D, Quyen DV, Singh NK, Kundumani-Sridharan V, Karpurapu M, Park EA, Glasgow WC, Rao GN. Src-dependent STAT-3-mediated expression of monocyte chemoattractant protein-1 is required for 15(S)-hydroxyeicosatetraenoic acid-induced vascular smooth muscle cell migration. *J Biol Chem*. 2009;284:31142–31155. doi: [10.1074/jbc.M109.012526](https://doi.org/10.1074/jbc.M109.012526)
33. Zhang B, Wu X, Liu J, Song L, Song Q, Wang L, Yuan D, Wu Z. β-Actin: not a suitable internal control of hepatic fibrosis caused by *Schistosoma japonicum*. *Front Microbiol*. 2019;10:66. doi: [10.3389/fmicb.2019.00066](https://doi.org/10.3389/fmicb.2019.00066)
34. Zhang Y, Wang H, Kovacs A, Kanter EM, Yamada KA. Reduced expression of Cx43 attenuates ventricular remodeling after myocardial infarction via impaired TGF-beta signaling. *Am J Physiol Heart Circ Physiol*. 2010;298:H477–H487. doi: [10.1152/ajpheart.00806.2009](https://doi.org/10.1152/ajpheart.00806.2009)
35. Spinale FG. Matrix metalloproteinases: regulation and dysregulation in the failing heart. *Circ Res*. 2002;90:520–530. doi: [10.1161/01.RES.0000013290.12884.A3](https://doi.org/10.1161/01.RES.0000013290.12884.A3)
36. Heymans S, Schroen B, Vermeersch P, Milting H, Gao F, Kassner A, Gillijns H, Herijgers P, Flameng W, Carmeliet P, et al. Increased cardiac expression of tissue inhibitor of metalloproteinase-1 and tissue inhibitor of metalloproteinase-2 is related to cardiac fibrosis and dysfunction in the chronic pressure-overloaded human heart. *Circulation*. 2005;112:1136–1144. doi: [10.1161/CIRCULATIONAHA.104.516963](https://doi.org/10.1161/CIRCULATIONAHA.104.516963)
37. Chin CWL, Shah ASV, McAllister DA, Joanna Cowell S, Alam S, Langrish JP, Strachan FE, Hunter AL, Maria Choy A, Lang CC, et al. High-sensitivity troponin I concentrations are a marker of an advanced hypertrophic response and adverse outcomes in patients with aortic stenosis. *Eur Heart J*. 2014;35:2312–2321. doi: [10.1093/eurheartj/ehu189](https://doi.org/10.1093/eurheartj/ehu189)
38. Li X, Lu Q, Qiu Y, do Carmo JM, Wang Z, da Silva AA, Mouton A, ACM O, Hall ME, Li J, et al. Direct cardiac actions of the sodium glucose co-transporter 2 inhibitor empagliflozin improve myocardial oxidative phosphorylation and attenuate pressure-overload heart failure. *J Am Heart Assoc*. 2021;10:e018298. doi: [10.1161/JAHA.120.018298](https://doi.org/10.1161/JAHA.120.018298)
39. Young LH, Zaha VG. AMP-activated protein kinase regulation and biological actions in the heart. *Circ Res*. 2012;111:800–814. doi: [10.1161/CIRCRESAHA.111.255505](https://doi.org/10.1161/CIRCRESAHA.111.255505)
40. Hasan R, Lasker S, Hasan A, Zerín F, Zamila M, Chowdhury FI, Nayan SI, Rahman MM, Khan F, Subhan N, et al. Canagliflozin attenuates isoprenaline-induced cardiac oxidative stress by stimulating multiple antioxidant and anti-inflammatory signaling pathways. *Sci Rep*. 2020;10:14459. doi: [10.1038/s41598-020-71449-1](https://doi.org/10.1038/s41598-020-71449-1)
41. Basu D, Huggins L-A, Scerbo D, Obunike J, Mullick AE, Rothenberg PL, Di Prospero NA, Eckel RH, Goldberg IJ. Mechanism of increased LDL and decreased triglycerides with SGLT2 inhibition. *Arterioscler Thromb Vasc Biol*. 2018;38:2207–2216. doi: [10.1161/ATVBAHA.118.311339](https://doi.org/10.1161/ATVBAHA.118.311339)
42. Andreadou I, Bell RM, Botker HE, Zurbier CJ. SGLT2 inhibitors reduce infarct size in reperfused ischemic heart and improve cardiac function during ischemic episodes in preclinical models. *Biochim Biophys Acta Mol Basis Dis*. 2020;1866:165770.

SUPPLEMENTAL MATERIAL

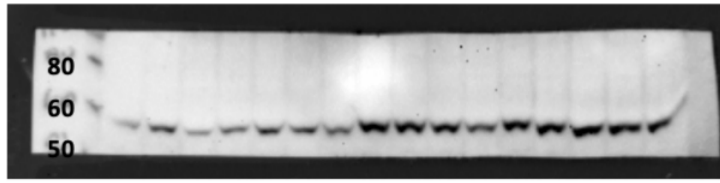
Table S1: Antibody Catalog Numbers

Antibody Name	Manufacturer	Catalog Number
Akt	Cell Signaling	9272
AMPK	Cell Signaling	2532
Angiostatin	Abcam	2904
Beta actin	Cell Signaling	4967
Connexin 43	Cell Signaling	83649
Desmin	Cell Signaling	4024
eNOS	Cell Signaling	32027
ERK1/2	Cell Signaling	4695
Filamin	Cell Signaling	4762
GAPDH	Cell Signaling	97166
Isolectin B4	Thermo Fisher Scientific	I32450
Jak2	Cell Signaling	3230
MCP-1	Cell Signaling	81559
MMP13	Cell Signaling	69926
mTOR	Cell Signaling	2972
p-Akt	Cell Signaling	4060
p-AMPK	Cell Signaling	2535
p-eNOS	Cell Signaling	9571
p-ERK1/2	Cell Signaling	4370
p-STAT3	Cell Signaling	9145
SMAD2/3	Cell Signaling	8685
SOD2	Cell Signaling	131415
STAT3	Cell Signaling	9139
TGFβ	Cell Signaling	3711
TIMP2	Cell Signaling	5738
Troponin I	Cell Signaling	13083
Troponin T	Cell Signaling	5593
Vimentin	Cell Signaling	5741
α-actinin	Cell Signaling	6487
α-fodrin	Cell Signaling	2122
α-SMA	Abcam	7817

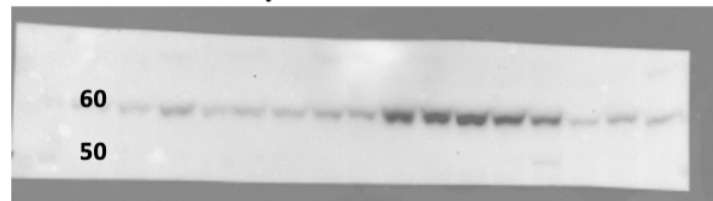
Antibodies used in this study are listed along with corresponding manufacturer and catalog numbers. AMPK, 5' adenosine monophosphate-activated protein kinase; eNOS, endothelial nitric oxide synthase; ERK, extracellular regulated kinase 1/2; GAPDH, glyceraldehyde-3-phosphate dehydrogenase; Jak2, janus kinase 2; MCP-1, monocyte chemoattractant protein-1; MMP13, matrix metalloproteinase 13; mTOR, mammalian target of rapamycin; p-, phosphorylated; STAT3, signal transducer and activator of transcription 3; SOD2; superoxide dismutase 2; TGFβ, transforming growth factor beta; TIMP2, tissue inhibitor of metalloproteinase 2; α-SMA, alpha smooth muscle actin.

FIGURE S1

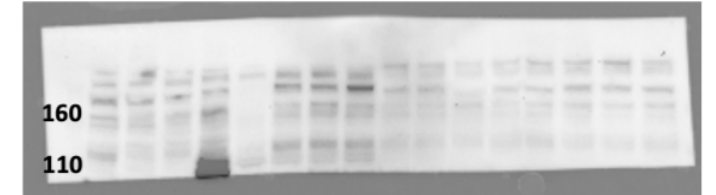
AMPK



p-AMPK



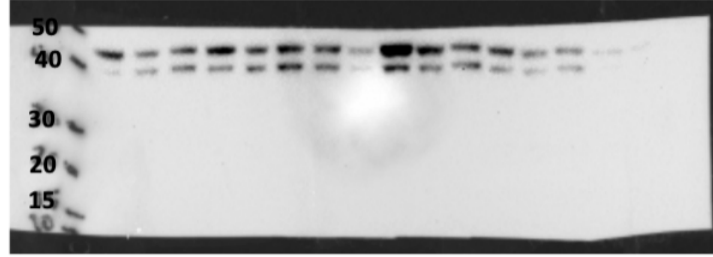
p-eNOS



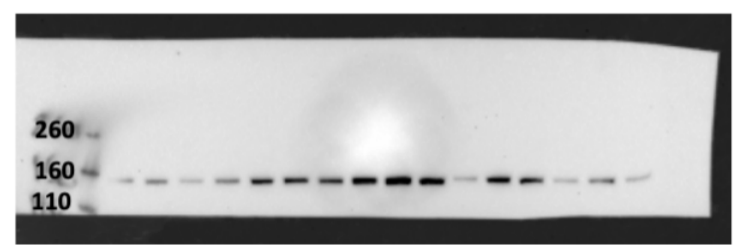
Total ERK1/2



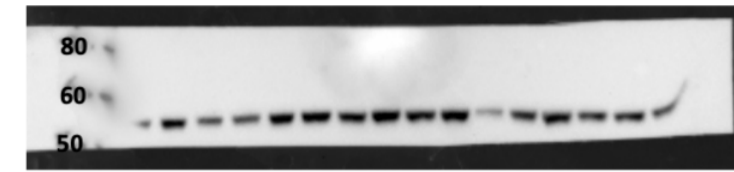
p-ERK1/2



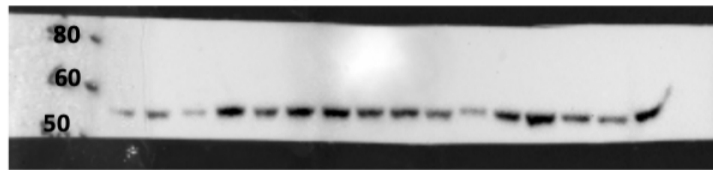
Total eNOS



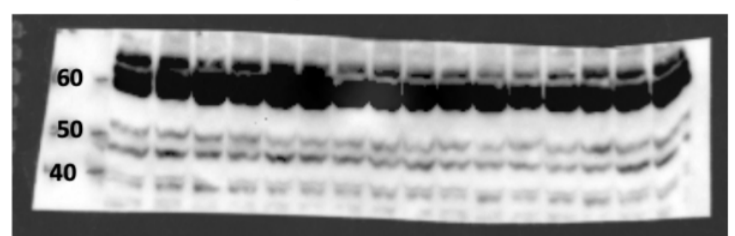
Total Akt



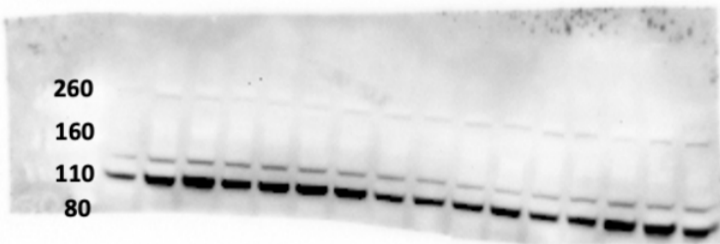
p-Akt



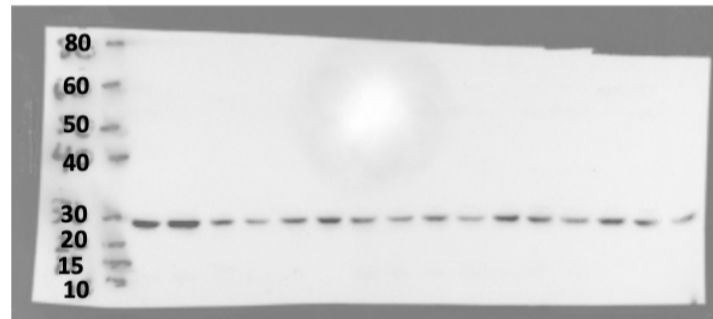
Angiostatin



Jak2



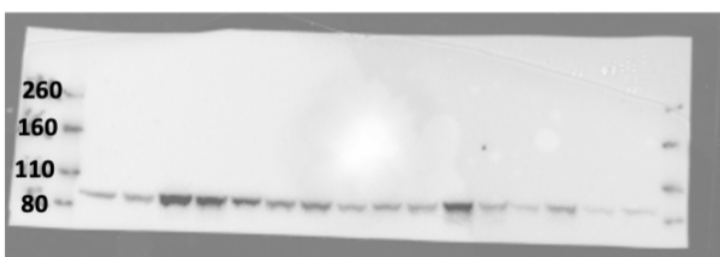
TGFβ



SMAD2/3



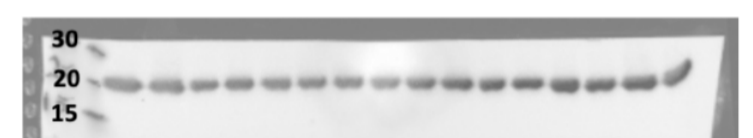
p-STAT3



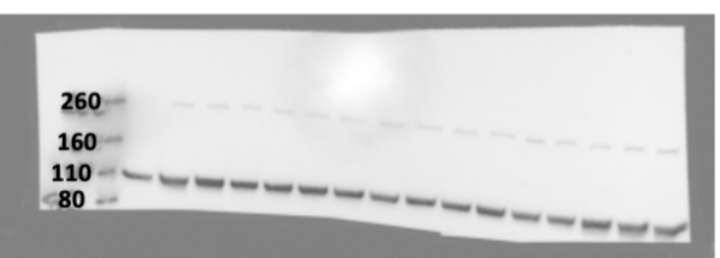
STAT3



SOD2



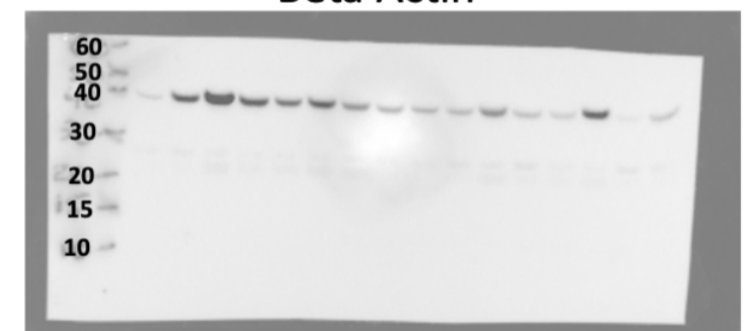
Alpha actinin



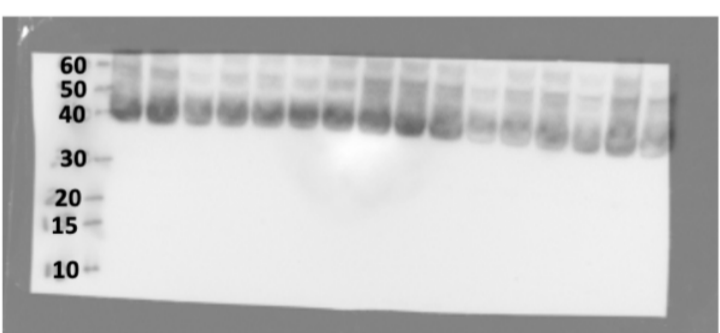
Alpha fodrin



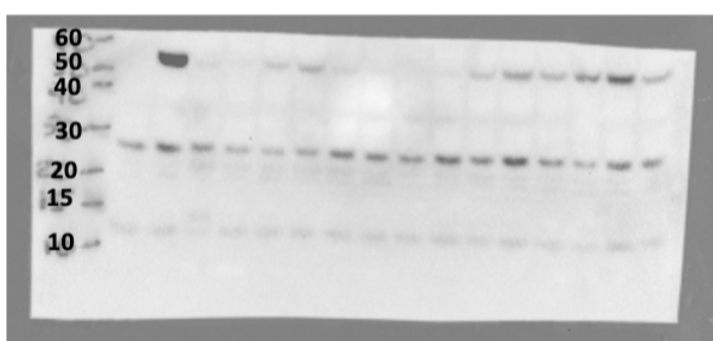
Beta Actin



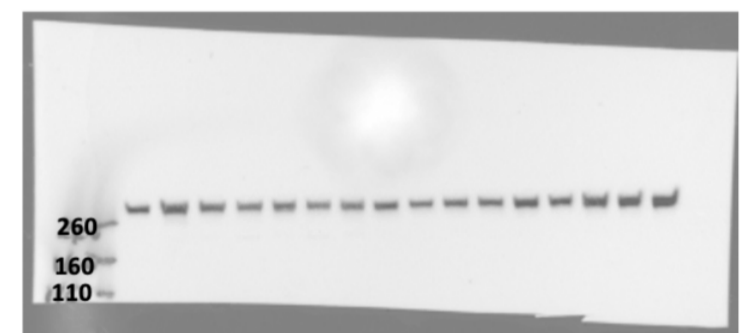
Connexin



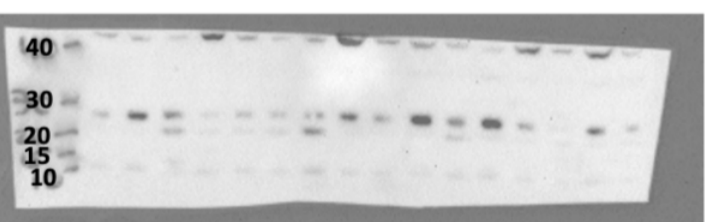
Desmin



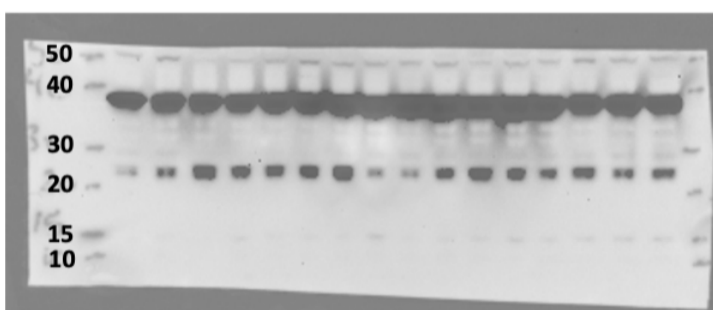
Filamin



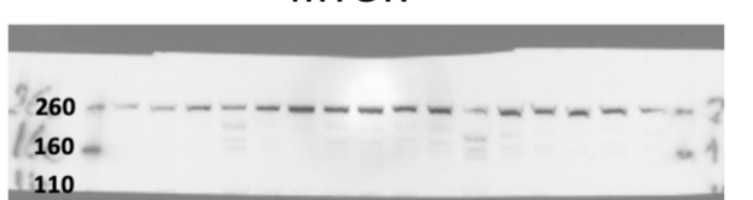
MCP-1



MMP13



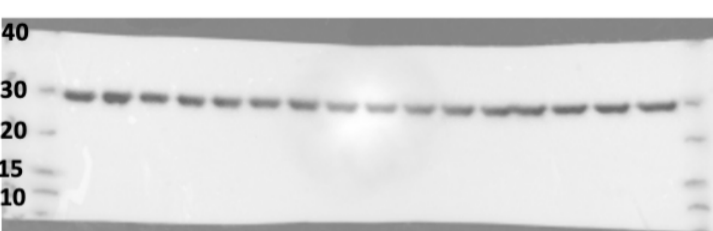
mTOR



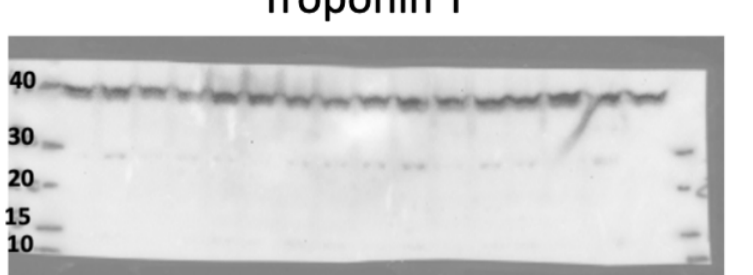
TIMP2



Troponin I



Troponin T



Vimentin



Figure S1: Immunoblot uncropped images. Uncropped immunoblot images with molecular weights (in kilodaltons) labeled on left. AMPK, 5' adenosine monophosphate-activated protein kinase; eNOS, endothelial nitric oxide synthase; ERK, extracellular regulated kinase 1/2; GAPDH, glyceraldehyde-3-phosphate dehydrogenase; Jak2, janus kinase 2; MCP-1, monocyte chemoattractant protein-1; MMP13, matrix metalloproteinase 13; mTOR, mammalian target of rapamycin; p-, phosphorylated; STAT3, signal transducer and activator of transcription 3; SOD2; superoxide dismutase 2; TGF β , transforming growth factor beta; TIMP2, tissue inhibitor of metalloproteinase 2.

FIGURE S2

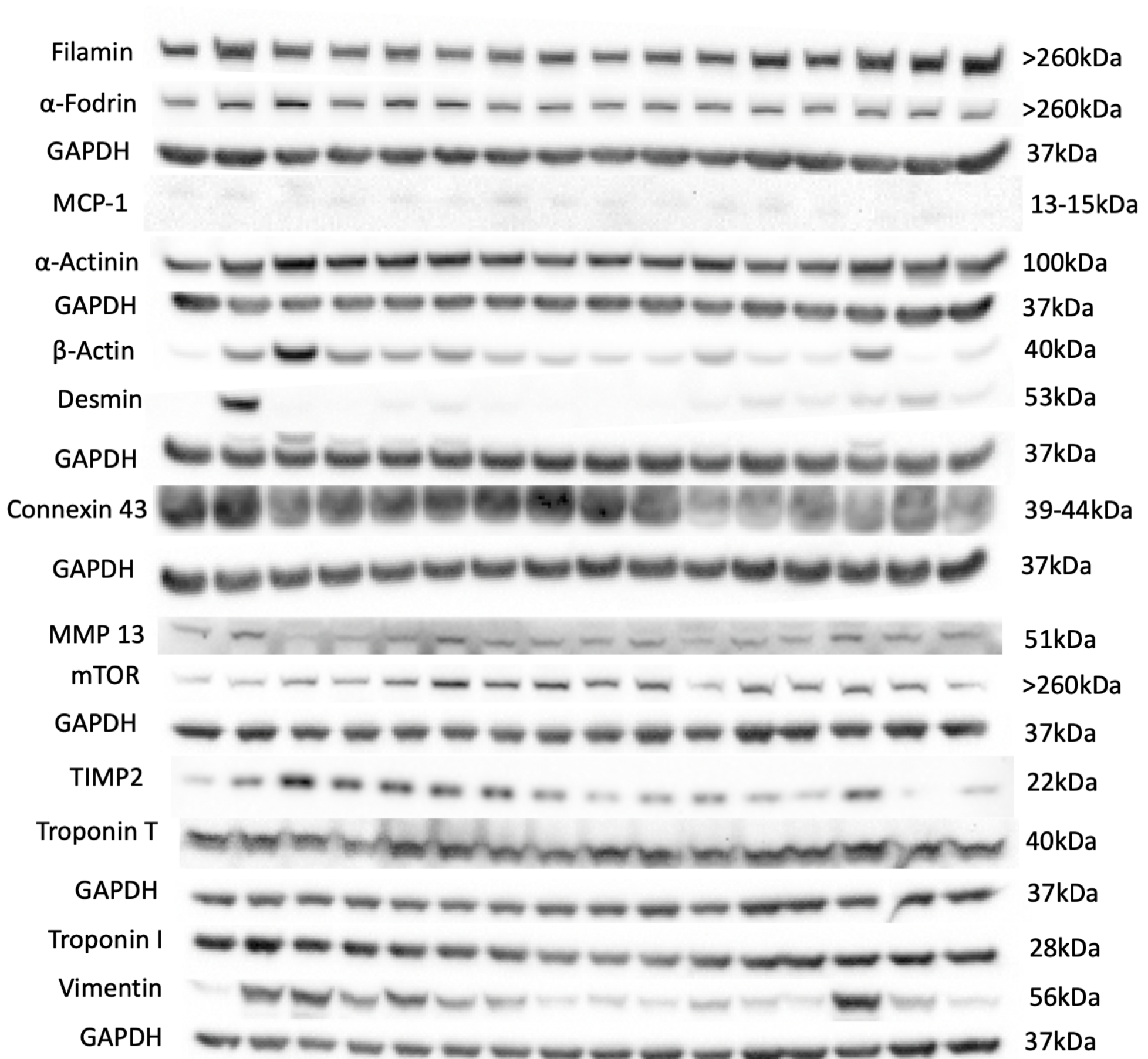
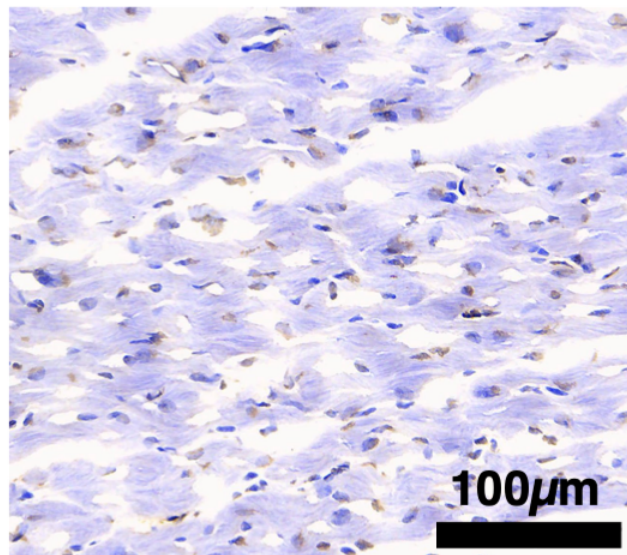
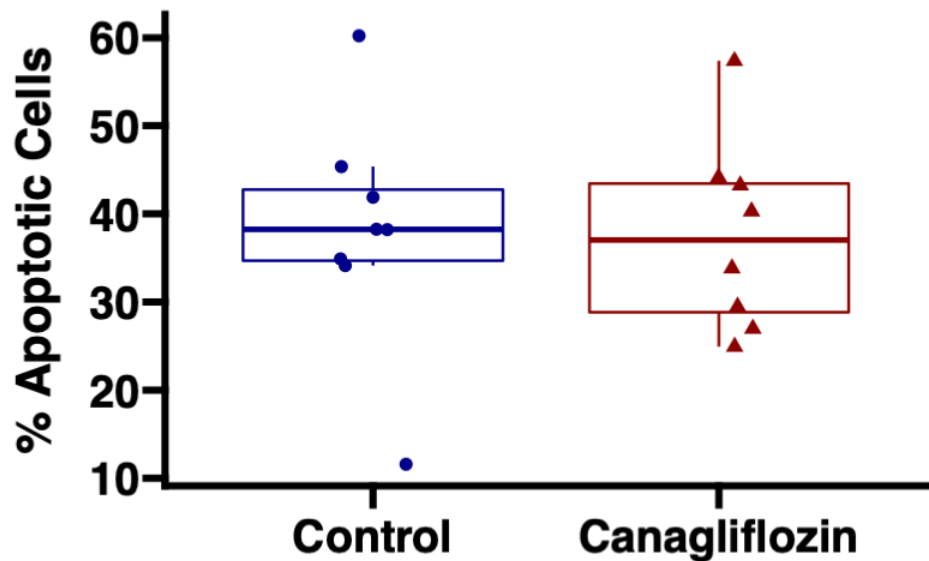


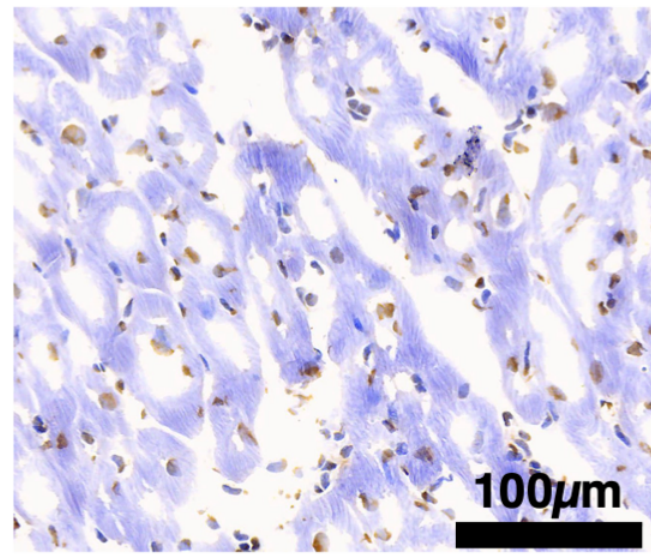
Figure S2: Fibrosis-related western blot bands. Complete western blot bands displayed for protein quantification. Bands were normalized to glyceraldehyde-3-phosphate dehydrogenase (GAPDH). MMP13, matrix metalloproteinase 13; TIMP2, tissue inhibitor of metalloproteinase 2; MCP-1, monocyte chemoattractant protein-1; mTOR, mammalian target of rapamycin.

FIGURE S3

TUNEL Staining



CON



CANA

Figure S3: Canagliflozin therapy has no effect on apoptosis in chronically ischemic myocardial tissue. There were no differences in percentage of apoptotic cells in ischemic myocardium as measured by terminal deoxynucleotidyl transferase dUTP nick end labeling (TUNEL) staining between canagliflozin-treated pigs (CANA, n=8) and control (CON, n=8). Representative images of TUNEL staining in ischemic myocardial tissue shown. Upper and lower borders of box represent upper and lower quartiles, middle horizontal line represents median, upper and lower whiskers represent maximum and minimum values.